DISTRIBUTION AND ORIGIN OF MID-CONTINENT PENNSYLVANIAN PHOSPHORITES

by

David Lee Kidder

A thesis submitted in partial fulfillment
of the requirements for the degree of
Master of Science in Geology
in the Graduate College of
The University of Iowa

July, 1982

Thesis supervisor: Professor Philip H. Heckel

Graduate College
The University of Iowa
Iowa City, Iowa

CERTIFICATE OF APPROVAL

MASTER'S THESIS

This is to certify that the Master's thesis of

David Lee Kidder

has been approved by the Examining Committee for the thesis requirement for the Master of Science degree in Geology at the July, 1982 graduation.

Thesis committee: Philip H Heckel
Thesis supervisor

Member

R. G. Baker
Member

ACKNOWLEDGMENTS

I wish to express thanks to Philip Heckel who served as thesis supervisor and introduced me to the field area. I also thank Keene Swett and Richard Baker who served as members of the thesis committee.

The Geology department at the University of Iowa provided the necessary laboratory facilities for this project. Financial support was awarded by the Kansas Geological Survey, the Oklahoma Geological Survey, and Sigma Xi. Maps were provided by the Kansas Geological Survey.

The kindness of the many landowners and quarry operators throughout the study area is greatly appreciated. John Malinky provided a wealth of phosphate nodules from Tyro Quarry. Special thanks to Mary Wyckoff who painstakingly edited and typed the manuscript.

ABSTRACT

Widespread, laterally continuous mid-continent Pennsylvanian black shales are characterized by nodular to laminar phosphorites. In general, larger nodules occur in the thicker black shales, while smaller nodules occur in thinner black shales. Nodule shape is related to geographic position, with nodules becoming progressively flatter from south to north.

Many phosphorite nodules contain abundant and diverse radiolarians. Peloids are also an abundant grain type, and pelagic megafossils (e.g. nautiloids and fish bones) occasionally are included in the nodules. Detrital material and terrestrial palynomorphs are virtually absent in the phosphorites.

The phosphorites formed by displacive growth below the sediment/water interface, and much of the apatite precipitated directly from the interstitial waters on radiolarian tests. Most of the phosphorus was probably supplied to the sediment through the breakdown of planktonic organisms and fecal material.

The close similarity between these Pennsylvanian phosphorites and certain aspects of modern phosphorites suggests that the Pennsylvanian phosphorites and enclosing shales probably formed very slowly (at rates on the order of a few millimeters of growth per thousand years) in an offshore, sediment-starved regime.

TABLE OF CONTENTS

LIST OF FIGURES

INTRODUCTION

The depositional environment of thin, widespread, black shales is perhaps the most controversial aspect of the Pennsylvanian cyclothems of mid-continent North America (Moore, 1929; Zangerl and Richardson, 1963; Evans, 1966; Schenk, 1967; Merrill, 1975; Wilson, 1975, Heckel, 1977). Phosphorites contained in the black and gray "core" shale facies (Figure 1) of Heckel (1977) preserve petrologic and paleontologic information regarding the origin of the black shales that is often obscured in the shales themselves.

Cook and McElhinny (1979) presented a plate tectonics model that explains the spatial and temporal distribution of phosphorites worldwide. The authors noted that phosphorites deposited in epicontinental seas have yet to be incorporated into their model. This probably reflects a lack of modern epicontinental sea phosphorites as well as a paucity of detailed studies of ancient ones.

This paper examines the nature of Middle and Upper Pennsylvanian epicontinental marine phosphorites from northeastern Oklahoma to south-central Iowa (Figure 2). Particular attention is paid to the type of phosphorite (nodular vs. laminar), size and shape distribution of phosphorite nodules, petrology of the phosphorite, and microbiota contained in the nodules and surrounding shales. Integration of this information into a model that explains the origin of the phosphorite

Figure 1. Idealized Kansas cyclothem. From Ravn (1981) after Heckel (1977). Member terminology after Moore (1936) and Heckel (1977).

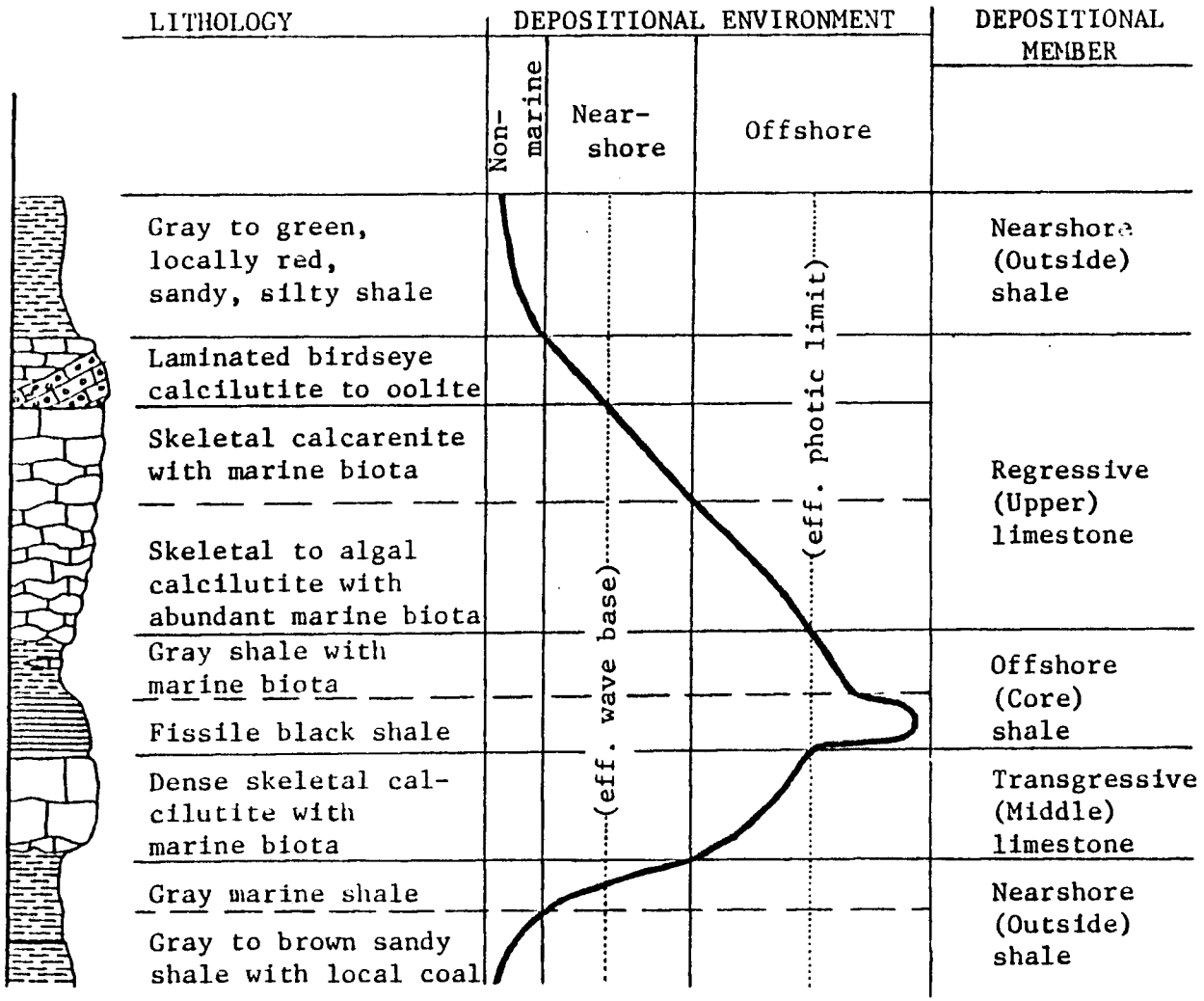

Figure 2. Paleotectonic features (after Moore, 1979), field area, and localities.

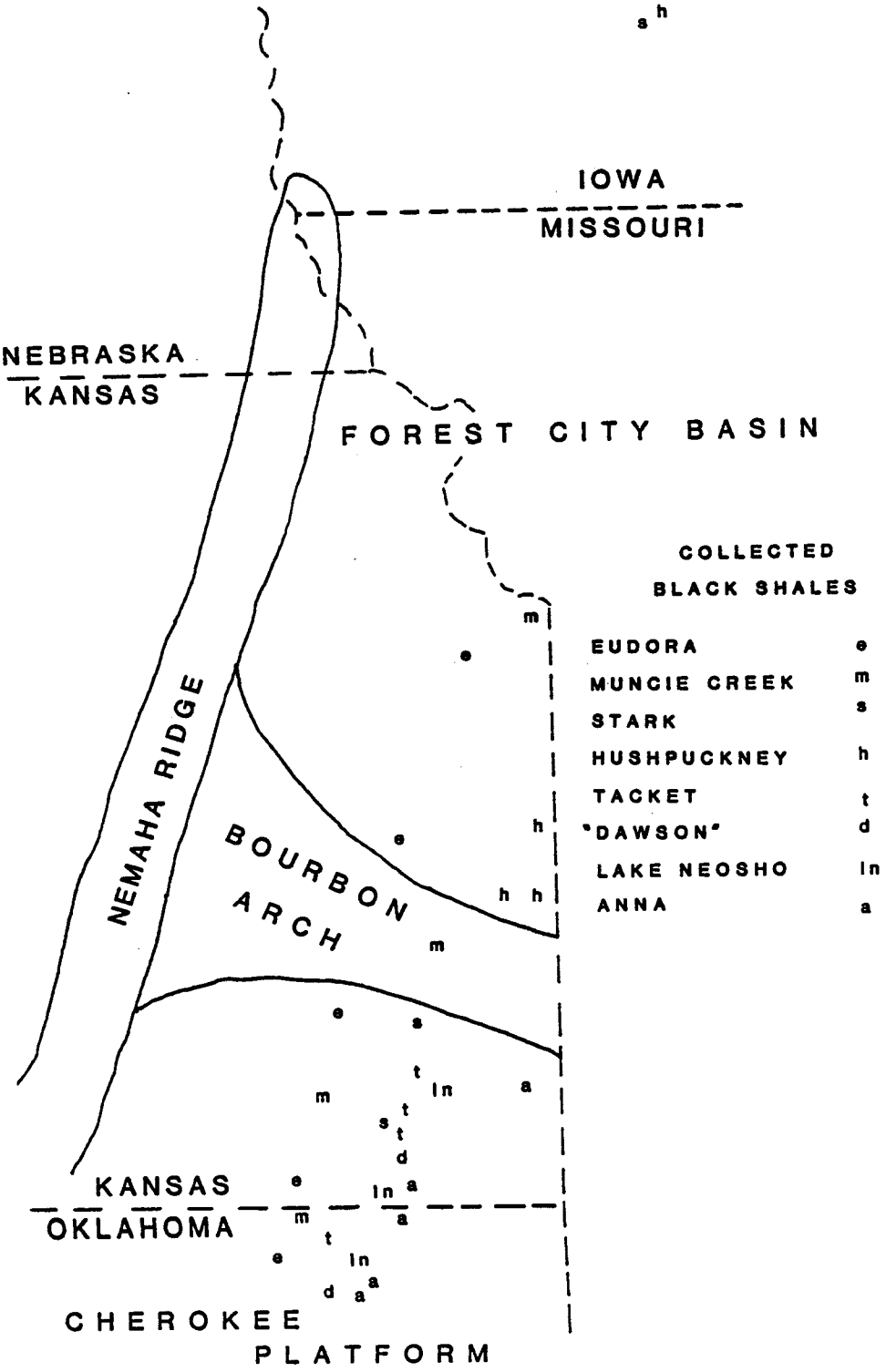

will not only strengthen our understanding of the black shale, but also will add to our understanding of the genesis of phosphatic sedimentary rocks.

Geologic Setting

The mid-continent Pennsylvanian outcrop belt extends from SSW to NNE, dipping slightly westward in an area that is largely undisturbed structurally. The Forest City basin and the Cherokee platform are the principle sedimentary basins in the study area (Moore, 1979). The most notable positive tectonic features are the Bourbon arch in the central portion of the outcrop belt and the Nemaha ridge to the west (Figure 2). Moore (1979) reported that the Cherokee platform dipped slightly to the south during Pennsylvanian time, but was generally stable tectonically. Major detrital sediment sources shifted from the northeast during the Middle Pennsylvanian to the south during the Upper Pennsylvanian.

The mid-continent Pennsylvanian sequence generally consists of alternating shales and limestones (Figure 3). The cyclic nature of the deposits has received a great deal of attention in the literature. The history of much of the study concerning this cyclicity has been reviewed by Ravn (1981), and the most recent account of the cyclicity is presented in Heckel's (1977) reinterpretation of Moore's (1936) Shawnee megacyclothem. The currently recognized Kansas cyclothem (Heckel, 1977) begins with a sandy, basal, nearshore (outside) shale, overlain by a thin transgressive limestone, followed by a thin gray to black offshore (core) shale, overlain by a thick regressive limestone followed by a higher nearshore shale that marks the beginning of a new

Figure 3. Generalized stratigraphic column of mid-continent Pennsylvanian after Heckel (1980). Symbols for sampling localities for each black shale are shown on left. Exact locations given in Appendix A. "Dawson" represents unnamed black shale above Dawson Coal.

Figure 3

Sampling localities

Iowa	Kansas	Oklahoma	Black Shale
	TyQ, NQEB, PtC, K-10	CpD	Eudora
	Neo, Ktl, K-32	Can	Muncie Creek
US-169	DSW, TS		Stark
IPP, IWS	K-52, NWD, US-69		Hushpuckney
	Wltn, PCC, K-57	OHC	Tacket
	MVSW	ODC	"Dawson"
	KBQ, NCSL	OWHB	Lake Neosho
	Els, JQ	OCBE, O-28, OBC	Anna

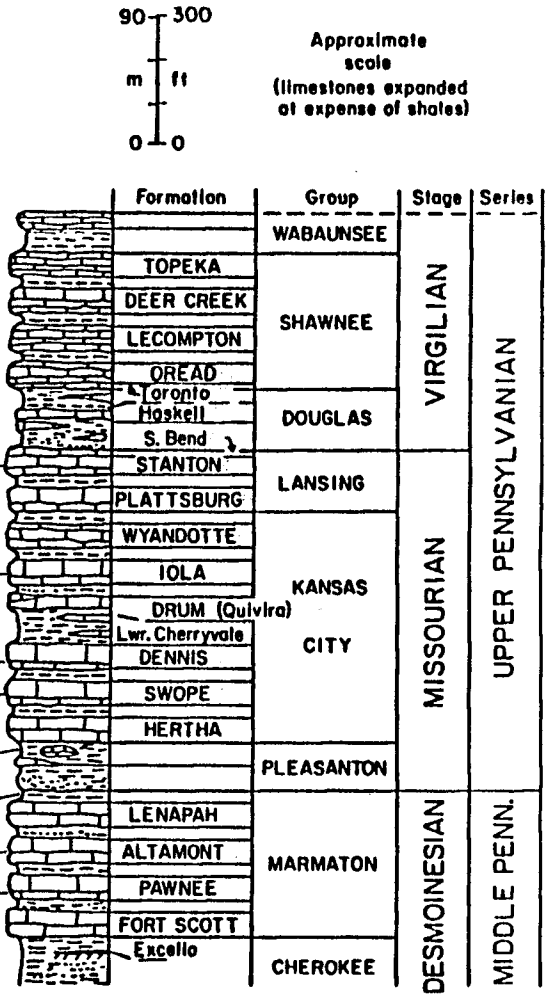

cycle (Figure 1). Wanless and Shepard (1936) and Heckel (1980) have suggested that eustatic sea level changes may account for the rapid cyclicity of the deposits, and Crowell (1978) has documented Late Paleozoic glaciations that may explain the eustatic changes.

Nodular to laminar phosphorite usually occurs in the black facies of the "core" shale of the cycle, but phosphorite nodules are often present in the gray facies as well.

Methods

Nodules and laminae of phosphorite and enclosing shales were sampled from eight shale horizons at thirty localities in Oklahoma, Kansas, and Iowa (Figure 3). The long, intermediate, and short axes of the nodules were measured using a vernier caliper prior to thin sectioning. Size variations among the three axes were compared using the "histogram" program contained in the Hewlett-Packard "HP-97 Stat-Pac."

Petrographic study was based on 101 thin sections of phosphorite nodules and three semi-impregnated thin sections of fissile black shale containing phosphorite laminae.

Thirty-one samples of enclosing shales were processed for palynomorphs following the format of Doher (1980). The process was discontinued after the hydrofluoric acid stage because most of the shales were barren, and recovery was extremely poor in the few samples that contained palynomorphs.

DISTRIBUTION OF PHOSPHORITE

Most of the non-skeletal phosphorite in the study area occurs as laminae and nodules. The presence or absence of laminae is often difficult to recognize in the field because visibility of laminae is largely controlled by the degree of weathering on outcrop. Laminae are present in outcrops both with and without nodules, and thus are not restricted in occurrence. Localities with phosphorite laminae alone are confined to the northeastern parts of the outcrop belt.

Nodules are generally confined to the central and southwestern portions of the outcrop belt. Variations in nodule size, shape, and abundance provided data for quantitative distribution analyses.

Abundance

Abundance of nodules is often difficult to ascertain as the quality of the exposure frequently biases the ease of collecting. Quantitative measure of abundance was possible at so few localities that only a rough qualitative method was utilized. Abundances were ranked as: high (H), moderate (M), low (L), very low (VL), and absent (A). High abundance means that the nodules were so conspicuous on outcrop that little or no digging was required for extraction. Low abundance means that nodules were scarce even with extensive digging. Moderate abundance encompasses everything

between high and low. Very low abundance means that extremely few nodules were found even with exhaustive digging.

Size

The long, intermediate, and short axes of 1012 phosphorite nodules were measured to observe trends in size and shape. For most localities, and at distinct levels within the shale for those localities at which detailed sampling was possible, the mean and standard deviation were calculated for each nodule dimension. Regional size comparisons were based upon an average of the mean sizes of all three parameters for a given population in order to minimize biases of shape in the size comparisons.

Shape

Shapes were analyzed by plotting the measured values of each nodule on Sneed and Folk's (1958) form classification diagram (Figure 4). Shape comparisons were carried out by modifying Sneed and Folk's terminology to create a hierarchical classification scheme. Spherical (S), bladed (B), platy (P), and elongated (E) were the end members used to derive a simple but informative means of comparing nodule shape throughout the study area. The method through which nodules were classified is presented in Appendix B. The nodule populations were classified in the following way: Each population received one to three letters based on percentages of nodules in each subdivision of the triangular diagram. The first character is the dominant shape component in the nodule population. Subsequent

Figure 4. Nodule shape classification diagram (modified from Sneed and Folk, 1958) used in this study. S = short axis, L = long axis, I = intermediate axis.

Figure 4

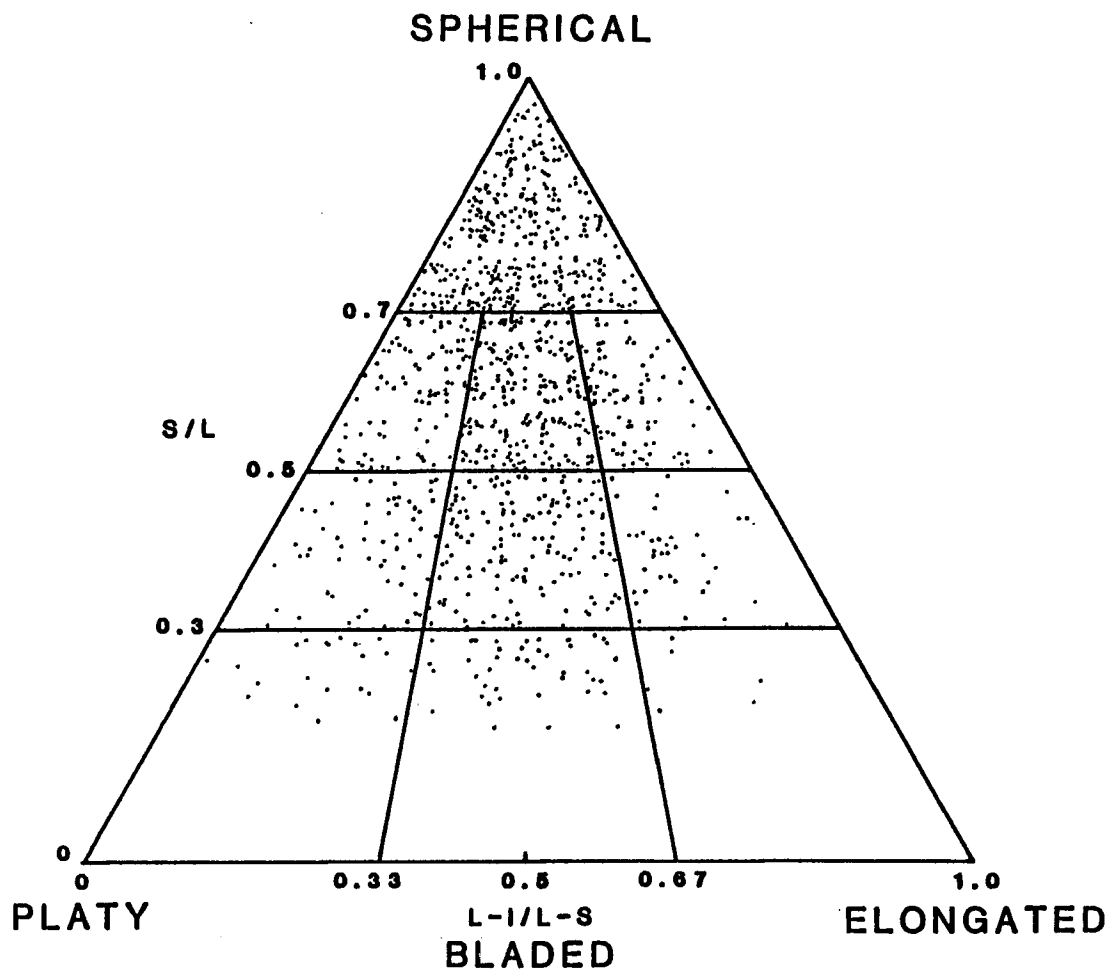

TOTAL NODULE POPULATION = SB

characters are end members that are significant, but not dominant, while characters in parentheses have even less importance. For example, SB(P) describes a population that consists largely of spherical nodules, but also contains a fairly high percentage of bladed forms, with a lower percentage of platy nodules present. The dominant shape range of all of the phosphorite nodules plotted together is SB (spherical-bladed) as shown in Figure 4.

Results

The following diagrams illustrate variations in size, shape, and abundance of nodules throughout the outcrop belt. The most significant trends relate to regional position and possibly to variations in paleotopography (as inferred from shale thickness), which, in some instances, can be related to the Bourbon arch (Figures 7, 8, and 12).

Histograms of nodule size variation in each dimension (long, intermediate, and short axes) usually display a positively skewed distribution. The short axis corresponds to the vertical dimension of nearly all of the nodules, suggesting that lateral growth was easier than vertical growth.

Average nodule size appears to have been influenced by shale thickness (Figure 5). Large nodules are much more abundant in thicker shales than in thin shales, perhaps as a result of sustaining a favorable environment for nodule formation for a longer period of time, or by providing more space for nodules to grow within the sediment. In general there is no clear relationship between nodule

Figure 5. Graph showing linear relationship between average nodule size and shale thickness. Each dot represents average size of a nodule population at localities where exposures permitted good thickness control. The Tacket Shale plots separately from other shales as it is generally much thicker than the other shales of this study. Solid lines represent calculated lines of best fit.

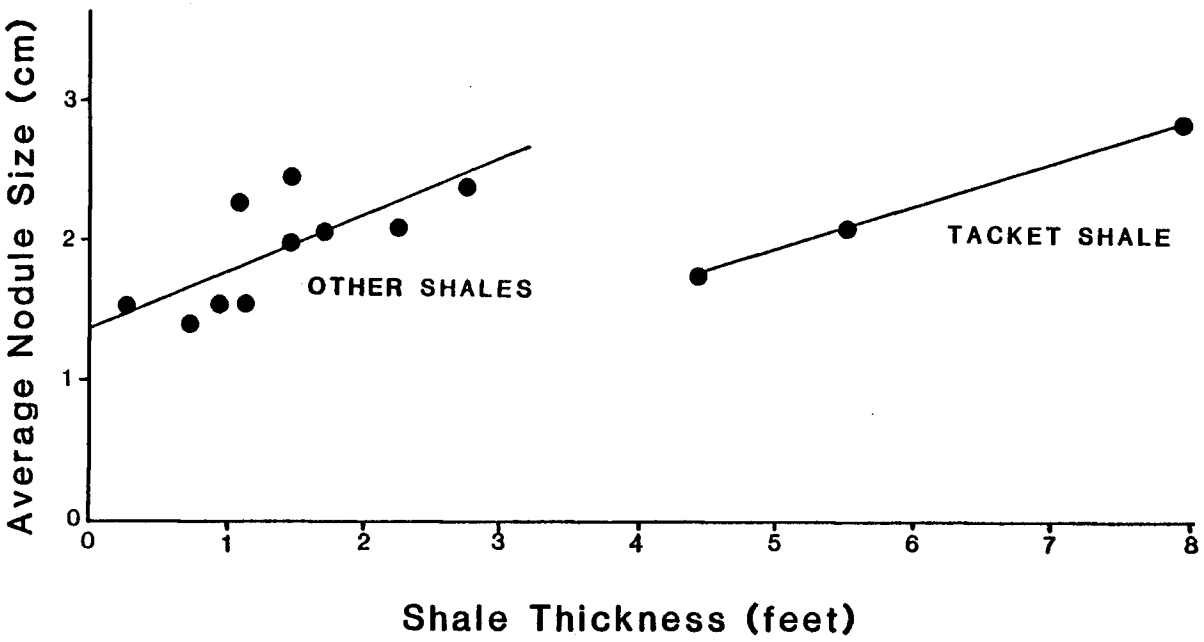

size and geographic position (Figure 6). The K-10 locality of the Eudora Shale, however, possesses the smallest nodules in the Eudora even though it is the thickest locality of the Eudora in this study (Figure 7). Much of the phosphorite at this locality is laminar, and the small nodules frequently grade laterally into laminae. The K-10 locality is in northeast Kansas, and the decrease in average nodule size at this locality may relate to increasing distance from the outlet to more open seaways that can be observed in Figure 10, and is discussed further under shape distribution.

Nodule shape seems to vary most noticeably on a regional basis (Figures 7, 8, and especially 9). Nodules in the southern part of the outcrop belt are spherical, grading northward into bladed forms, and finally becoming platy in northeastern Kansas and Missouri. Nodules are generally absent in Iowa, where non-skeletal phosphorite occurs principally as laminae or is absent.

The northward decrease in nodule size (in northeastern Kansas and Missouri) and relative nodule thickness (throughout the study area) could reflect a decreasing supply of available phosphorus, or a weakening in one or more of the mechanisms that may have been operating to concentrate phosphorus, possibly relating to increasing distance from the outlet of the mid-continent seas, which is illustrated in Figure 10. There does not appear to be any clear relationship between size and shape of nodules (Figure 11).

The only conspicuous trend in abundance may relate to the Bourbon arch. The regional picture (Figure 12) with regard to the Eudora and

Figure 6. Graph of average nodule size plotted against distance. Each dot represents average size of a nodule population at a given locality. 0 (distance) = southernmost locality near Nowata, Oklahoma.

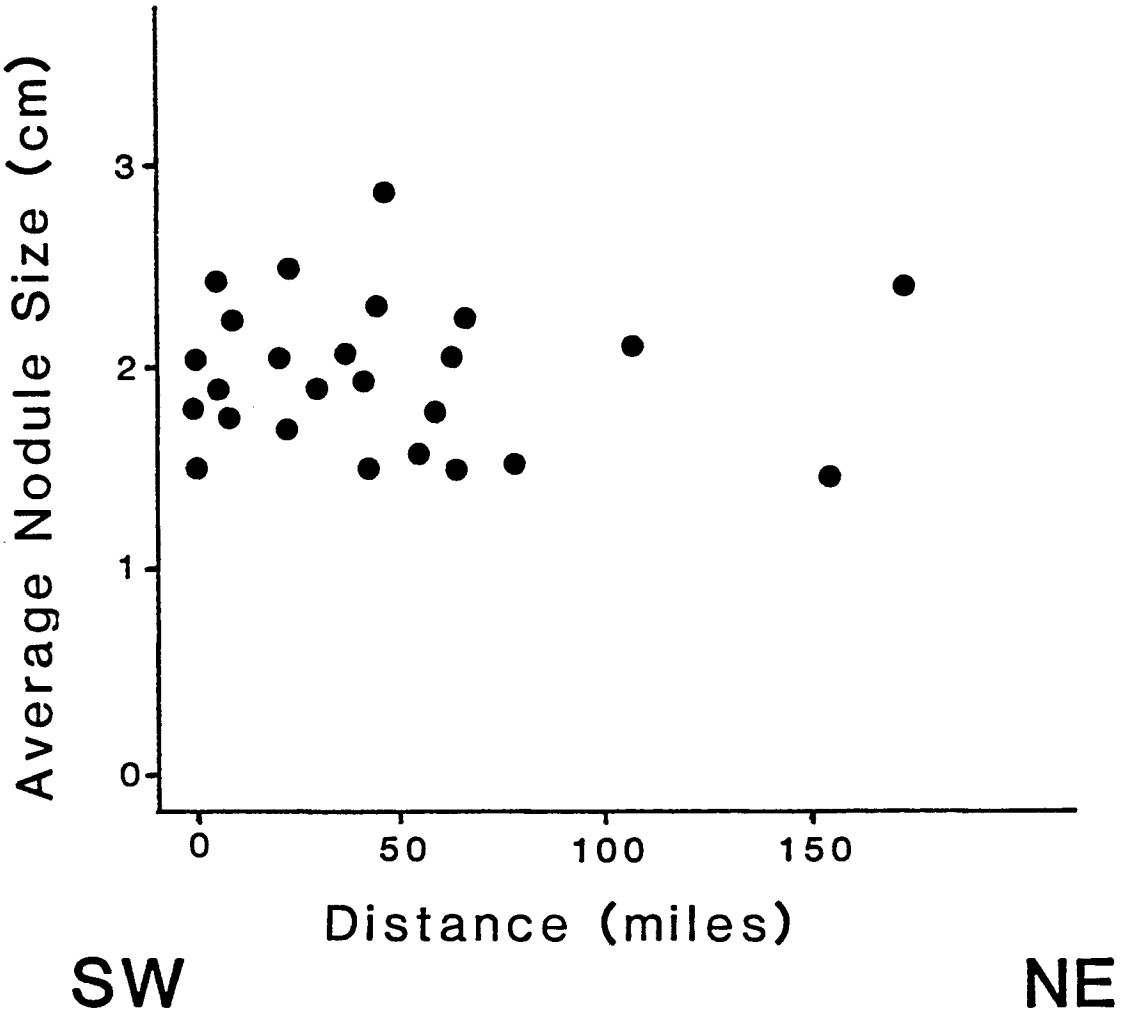

Figure 7. Size, shape, and abundance of nodules compared with "core" shale thickness. N(meas.) is number of nodules measured and is not directly related to outcrop abundance. Question marks indicate shales where only a minimum thickness is known.

a. Eudora Shale

b. Muncie Creek Shale

c. Stark Shale

d. "Dawson" Shale

Figure 7

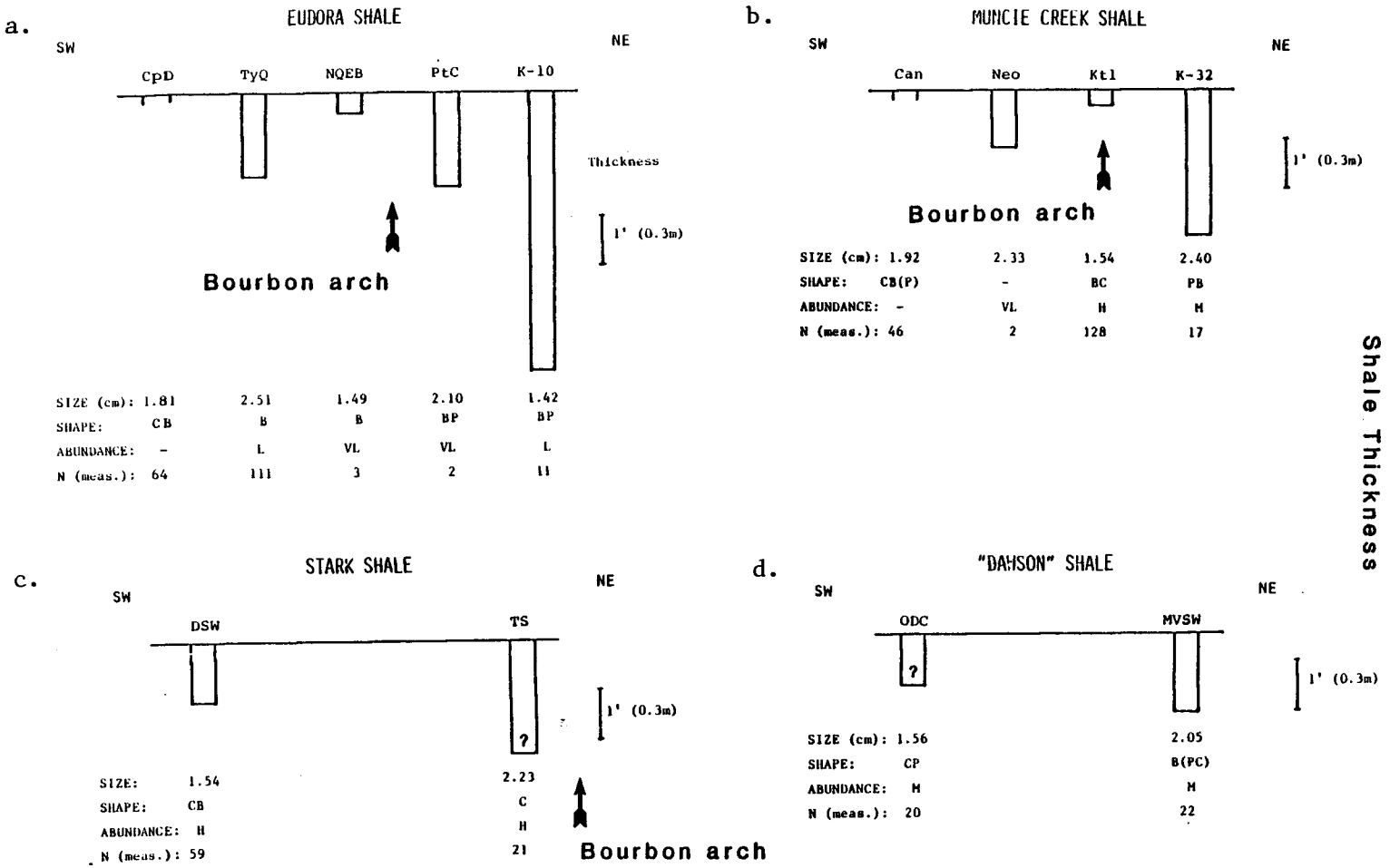
a.
EUDORA SHALE
SW
NE
CpD
TyQ
NQEB
PtC
K-10
Thickness
1' (0.3m)
Bourbon arch
SIZE (cm): 1.81 2.51 1.49 2.10 1.42
SHAPE: CB B B BP BP
ABUNDANCE: - L VL VL L
N (meas.): 64 111 3 2 11
b.
MUNCIE CREEK SHALE
SW
NE
Can
Neo
Ktl
K-32
1' (0.3m)
Bourbon arch
SIZE (cm): 1.92 2.33 1.54 2.40
SHAPE: CB(P) - BC PB
ABUNDANCE: - VL H H
N (meas.): 46 2 128 17
c.
STARK SHALE
SW
NE
DSW
TS
1' (0.3m)
?
SIZE: 1.54 2.23
SHAPE: CB C
ABUNDANCE: H H
N (meas.): 59 21
Bourbon arch
d.
"DAHSON" SHALE
SW
NE
ODC
MVSW
1' (0.3m)
?
SIZE (cm): 1.56 2.05
SHAPE: CP B(PC)
ABUNDANCE: H H
N (meas.): 20 22
Shale Thickness

Figure 8. Size, shape, and abundance of nodules compared with "core" shale thickness. N(meas.) is number of nodules measured and is not directly related to outcrop abundance. Question marks indicate shales where only a minimum thickness is known. Contradictions to size trends mentioned in text with regard to Anna and Lake Neosho Shales may relate to poorly known shale thicknesses.

a. Lake Neosho Shale

b. Anna Shale

c. Tacket Shale

Figure 8

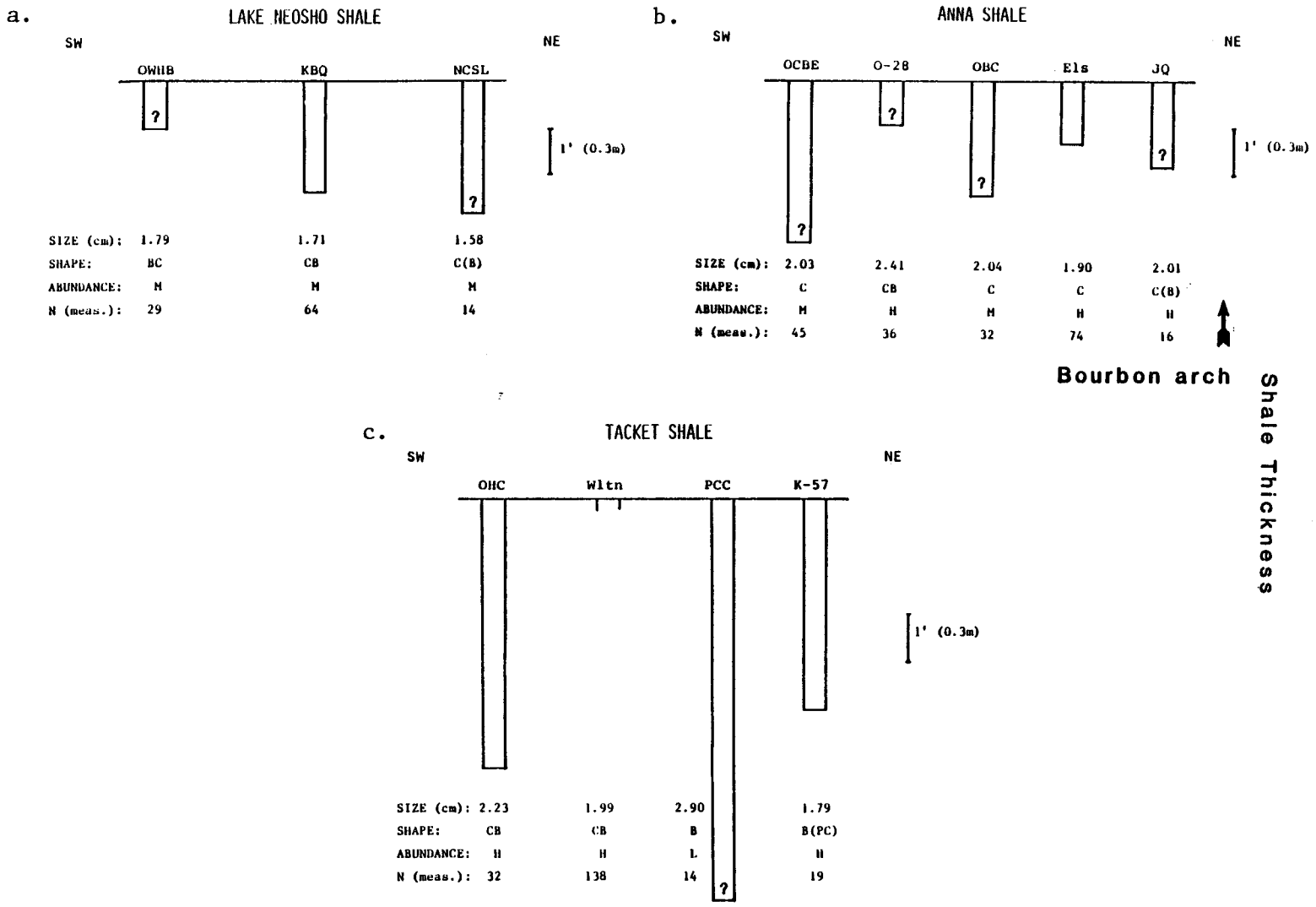
a.
LAKE NEOSHO SHALE
SW
NE
OWHB
KBQ
NCSL
?
?
?
1' (0.3m)
SIZE (cm): 1.79 1.71 1.58
SHAPE: BC CB C(B)
ABUNDANCE: M M M
N (meas.): 29 64 14
b.
ANNA SHALE
SW
NE
OCBE
O-28
OBC
Els
JQ
?
?
?
?
?
1' (0.3m)
SIZE (cm): 2.03 2.41 2.04 1.90 2.01
SHAPE: C CB C C C(B)
ABUNDANCE: M H M H H
N (meas.): 45 36 32 74 16
Bourbon arch
Shale Thickness
c.
TACKET SHALE
SW
NE
OHC
Wltn
PCC
K-57
?
1' (0.3m)
SIZE (cm): 2.23 1.99 2.90 1.79
SHAPE: CB CB B B(PC)
ABUNDANCE: H H L H
N (meas.): 32 138 14 19

Figure 9. Graph showing linear relationship between nodule shape and geographic position. Each dot represents average shape of a nodule population at a given locality. 0 (distance) = southernmost locality near Nowata, Oklahoma. Shape axis is semi-quantitative as explained in Appendix B. Solid line is calculated line of best fit. Dashed lines illustrate localities in Eudora and Muncie Creek Shales, which have the most complete sampling distribution.

Figure 9

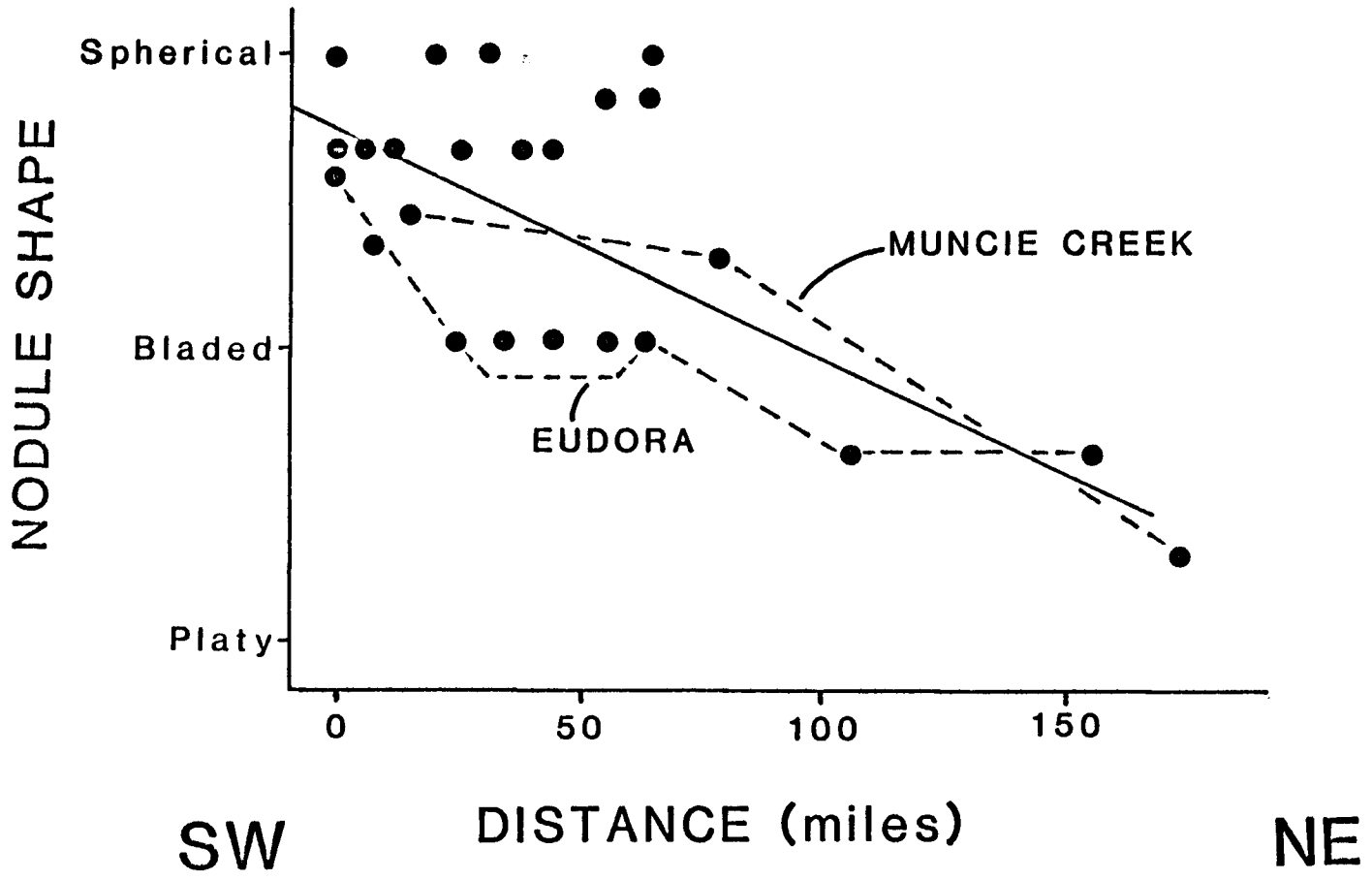
Spherical
Bladed
Platy
NODULE SHAPE
MUNCIE CREEK
EUDORA
0
50
100
150
SW
DISTANCE (miles)
NE

Figure 10. Upper Pennsylvanian paleogeography of the central United States. From Heckel (1980). Arrow "a" = general trend of Upper Pennsylvanian deep currents. Arrow "b" = general trend of Middle Pennsylvanian deep currents (P.H. Heckel, pers. comm., 1982). Prodeltaic area through which current "b" flowed was often covered by black shale during Middle Pennsylvanian.

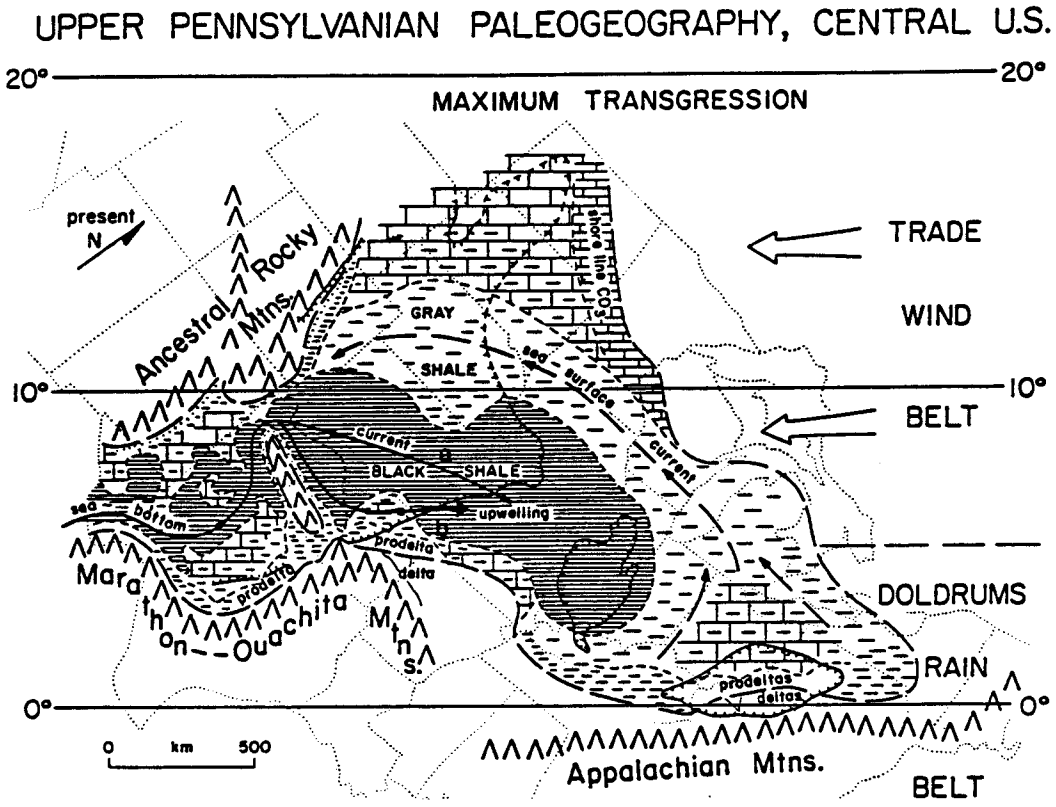

Figure 11. Graph of average nodule size vs. nodule shape. Each dot represents size vs. shape at a given locality. Shape axis is semi-quantitative as explained in Appendix B.

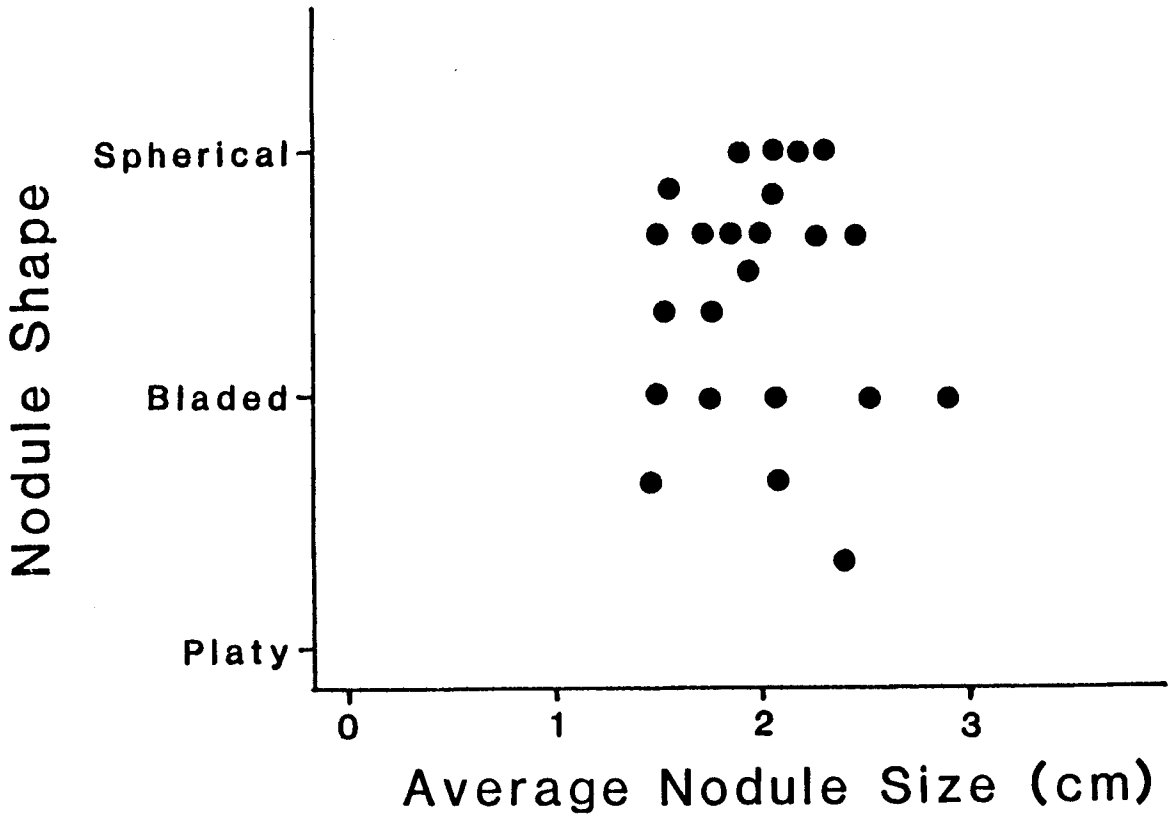

Figure 12. Nodule abundance across Bourbon arch in Eudora and Muncie Creek Shales. H = high abundance, VL = very low abundance.

Figure 12

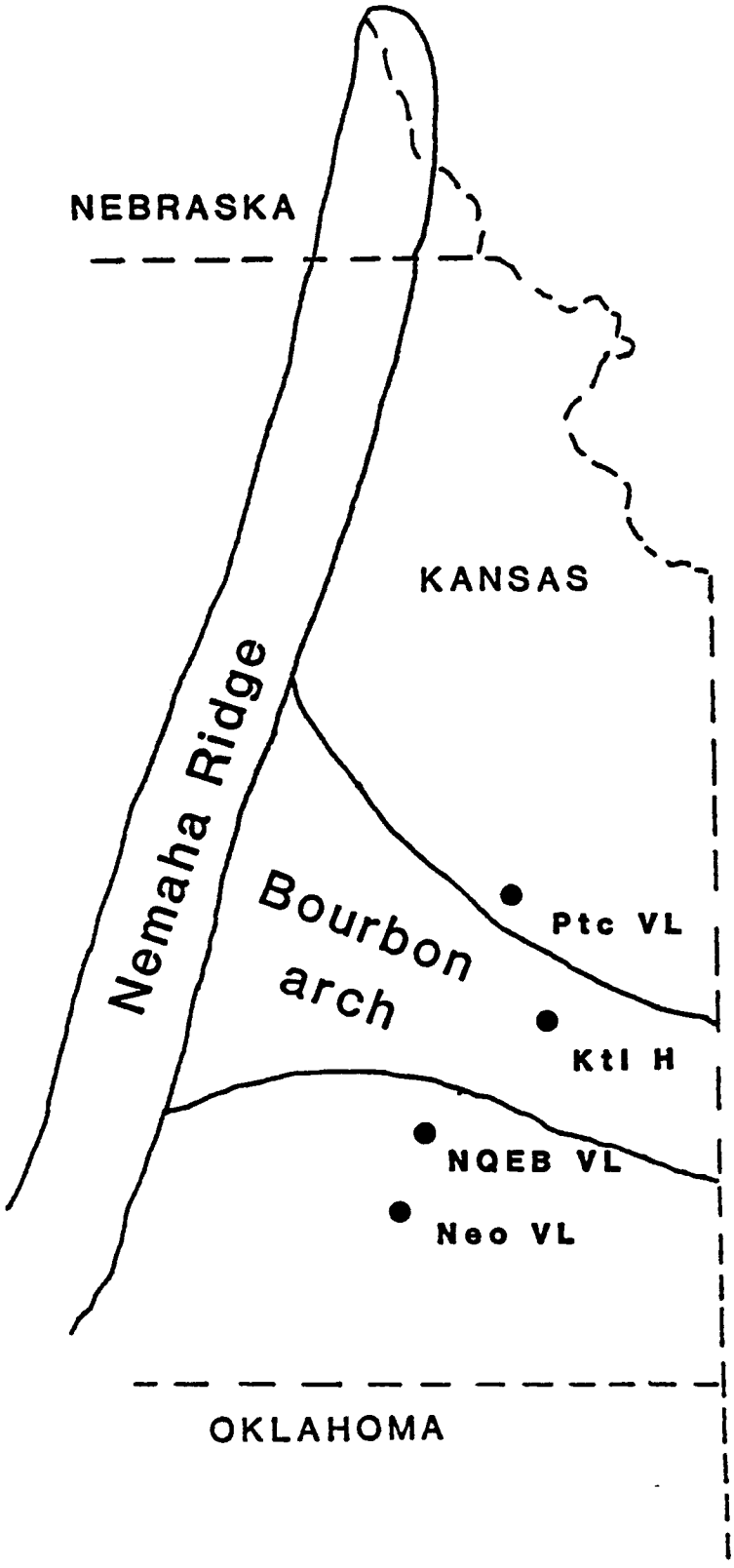
NEBRASKA
KANSAS
Nemaha Ridge
Bourbon arch
Ptc VL
Ktl H
NQEB VL
Neo VL
OKLAHOMA

Muncie Creek Shales, shows that on the flanks of the arch (PtC, NQEB, and Neo), nodule abundance is extremely low. On top of the arch (Ktl), abundance is very high. This increase in the relative amount of nodules on the arch could have resulted from winnowing of the surrounding sediment by bottom currents. Phosphorite nodules on the flanks of the arch may have been protected from such currents. It is also instructive to note that the Muncie Creek Shale is only three inches thick at Ktl (Figure 7b), and the shale is gray at this locality.

It appears that the Bourbon arch influenced patterns of phosphorite formation. Further study relating general trends in size, shape, and abundance to the Bourbon arch is needed to elucidate the manner in which the Bourbon arch affected the distribution of mid-continent Pennsylvanian phosphorites.

Vertical Variation

Only a few localities afforded detailed study of nodule variation vertically within a given shale. Nodules are often confined to a very narrow horizon near the top of the black shale, but some localities contain numerous discrete horizons throughout the shale. Els (Anna) and MVSW ("Dawson") provided the best opportunities to study variation within the shale. Rough qualitative measures performed at NCSL (Lake Neosho) and OHC (Tacket) show a general increase in nodule size toward the top of the black shale.

Figure 13 illustrates how nodule size varies vertically within two of the shales. Levels that exhibit larger nodules imply longer

Figure 13. Nodule size distribution within two black shales. Localities Els (Anna Shale) and MVSW ("Dawson" Shale) show two patterns of size change within shale, with larger nodules occurring near the upper (and sometimes lower) contacts of the shale. Sizes are represented by mean values from each sampling horizon (dots).

Figure 13

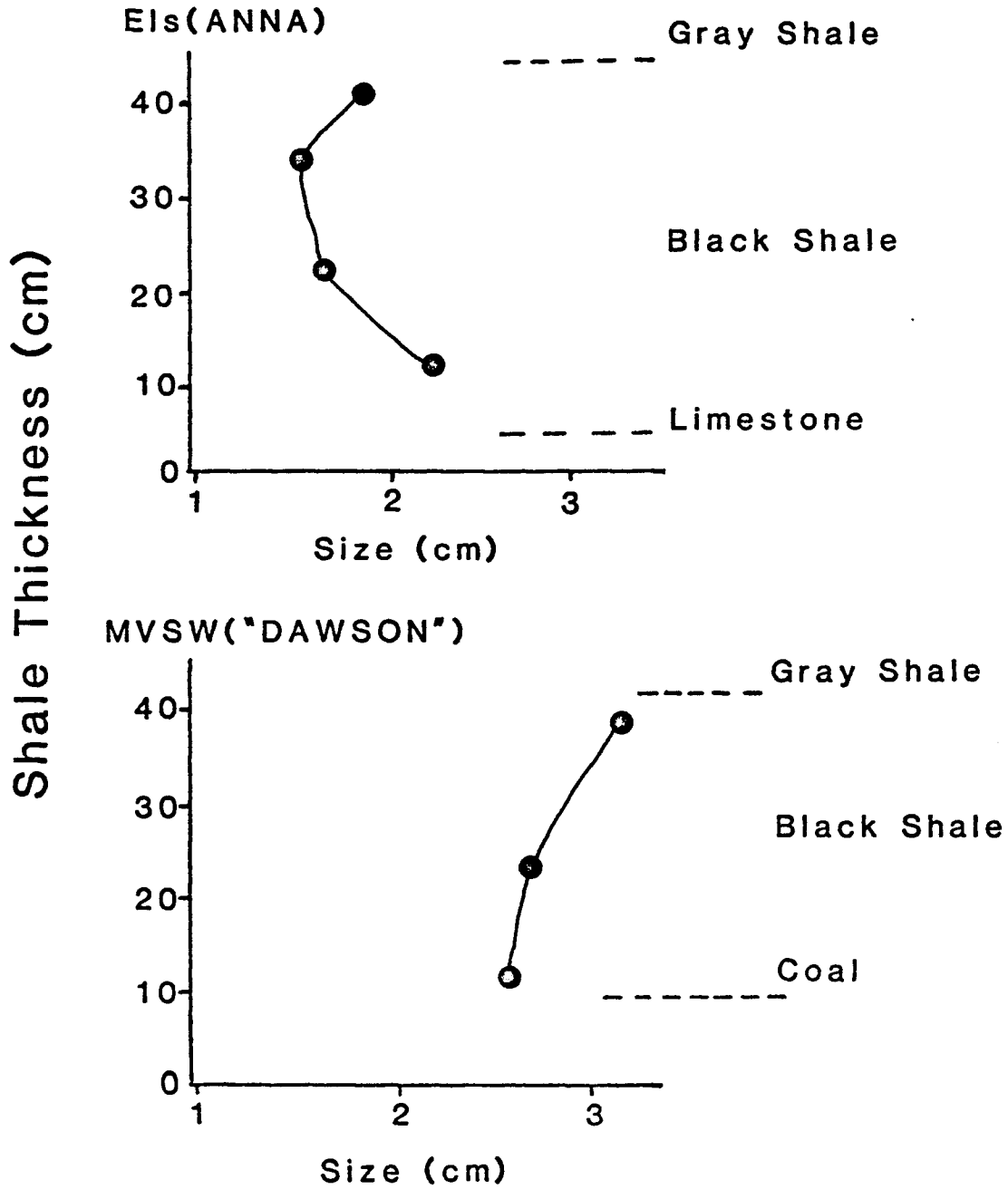
Shale Thickness (cm)
Els(ANNA)
Gray Shale
Black Shale
Limestone
40
30
20
10
0
1
2
3
Size (cm)
MVSW("DAWSON")
Gray Shale
Black Shale
Coal
40
30
20
10
0
1
2
3
Size (cm)

periods during which optimum conditions for growth of phosphorite nodules prevailed. Locality Els contrasts with this trend as the maximum size is attained near the base of the shale (Figure 13) but after reaching a low in about the middle of the shale, size increases again toward the top.

Modern phosphorites off the coast of Peru seem to form preferentially near the upper and lower boundaries of the oxygen minimum zone (Burnett and Veeh, 1977; Burnett et al., 1980; Burnett et al., 1982). The close association between large Pennsylvanian nodules and the upper and sometimes lower boundaries of the black shales suggests that phosphorite formation may have been facilitated at the boundaries of an oxygen minimum zone in the Pennsylvanian seaways of the mid-continent.

Stratigraphic Variation

Fluctuations in nodule size with time (Figure 14a) may be related mostly to average thickness of the shales. The Tacket shale is the thickest of the shales and contains the largest nodules. Nodule shape varies little stratigraphically, except in the youngest shales of this study where nodules appear to be generally flatter than in older shales (Figure 14b). Stratigraphic variations in both size and shape could be controlled at least in part by variations in the overall geometry of the depositional basin in which each shale was deposited. In particular, variation in water depth in individual cyclothems may have influenced circulation patterns in such a way as to affect phosphorite formation.

Figure 14. Stratigraphic variation of size and shape. Dots represent average size or shape for all localities sampled from each shale.

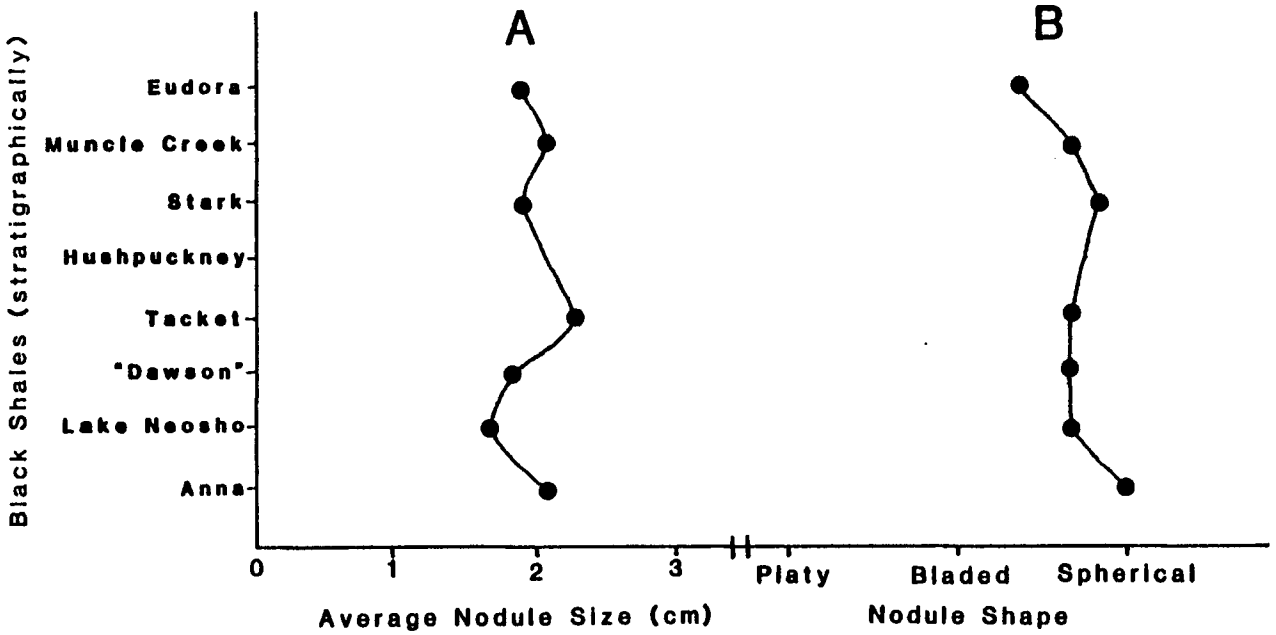

PETROLOGY

Non-skeletal phosphorite occurs principally as nodules and laminae. The nodules occur at distinct horizons probably representing periods when conditions favored phosphorite formation.

Growth of phosphorite nodules and laminae appears to have been largely displacive (Figure 15a, b, c). Figure 15a shows that the shale surrounding the nodule has been displaced. Although this relationship could have resulted from compaction of the shale around the nodule, Figure 15b provides more convincing evidence of displacive growth. Thin, wispy stringers of shale that have been displaced by growth of phosphorite are clearly visible in the outer portions of the nodule.

Most nodules show no internal structure, but occasional nodules exhibit concentric structure, and others display crude horizontal laminations. The horizontal laminations of phosphorite alternate with wispy stringers of shale, but concentrically laminated nodules generally do not display the wispy shale layers. Variations in internal structure of nodules could be related to growth rate.

Nodules

The phosphorite nodules are composed of peloids (Figure 15d), cements (apatite, calcite, silica, and pyrite), microfossils (radiolarians and tiny organic-walled spheroids), and various types of megafossils (nautiloids, inarticulate brachiopods, fish bones, and

Figure 15. Photomicrographs of phosphorite nodules.

a. Relationships between a phosphorite nodule and surrounding shale. Arrows denote where nodule protuberances have disturbed shale laminations. Nodule is from Lake Neosho Shale at locality KBQ. Bar scale = 600 microns. Plane polarized light.

b. Displacive relationships between a phosphorite nodule and enclosing shale. Arrow denotes wispy shale layers that have been displaced by nodule growth. Nodule is from Eudora Shale at locality K-10. Bar scale = 200 microns. Plane polarized light.

c. Shale containing phosphorite laminae consisting of micronodules. The white "laminae" represent artificial void space created during impregnation of shale. Laminations are oriented vertically in this photomicrograph to show more lateral extent of individual laminae. Sample is from Eudora Shale at locality K-10. Bar scale = 500 microns. Plane polarized light.

d. Collophane peloids in a phosphorite nodule from Lake Neosho Shale at locality OWHB. Bar scale = 150 microns. Plane polarized light.

Figure 15

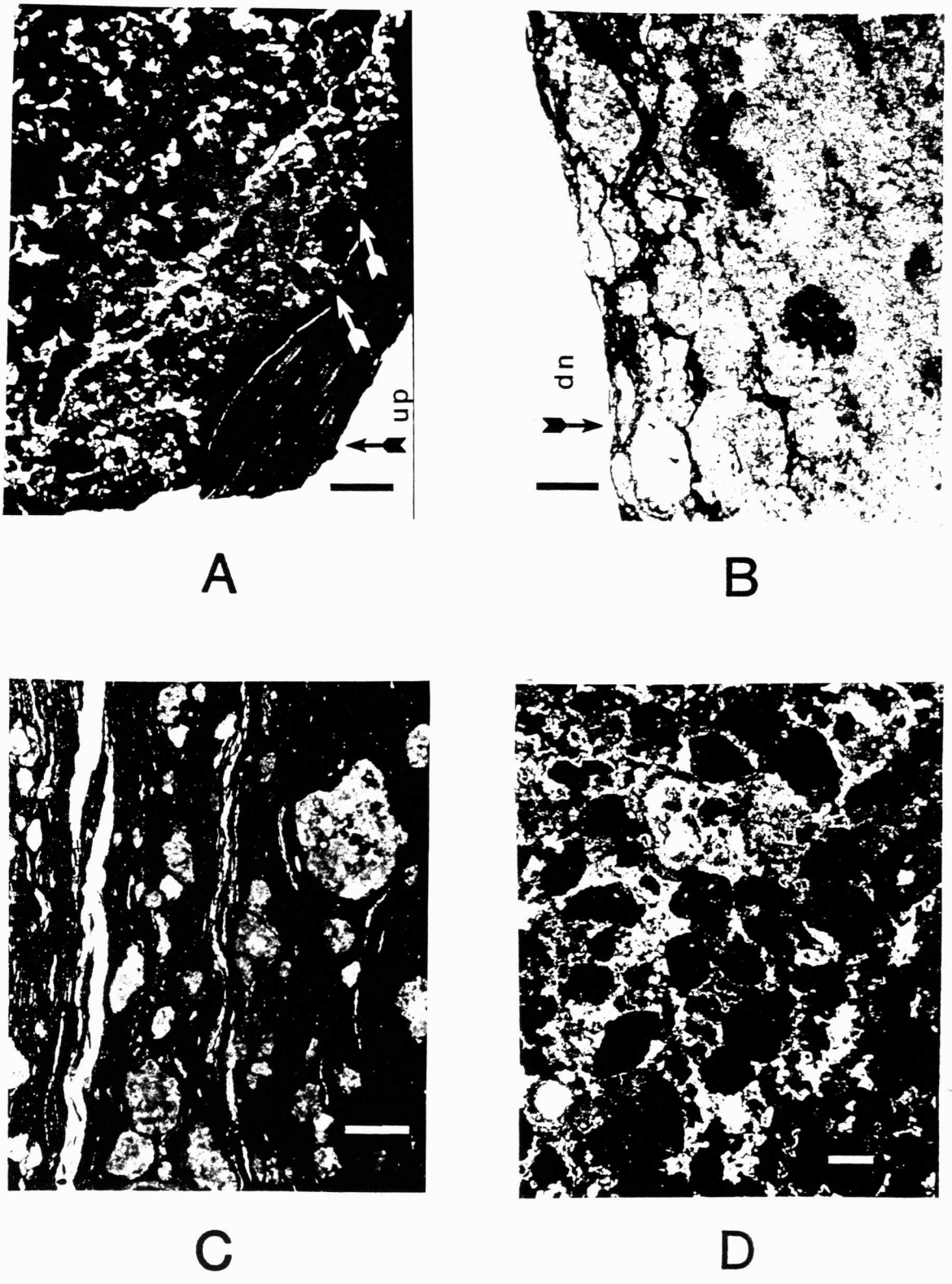

vascular plant debris). X-ray analyses (Runnels et al., 1953; Mitchell, 1981) show that the phosphorite in the nodules is a carbonate fluorapatite. The nodules generally average about thirty per cent P_2O_5 (Runnels et al., 1953). Detrital quartz is virtually absent in these nodules, and for that matter, in the surrounding shales as well.

Some nodules (particularly in the gray shales) are tightly packed calcarenites consisting of invertebrate skeletal debris. These carbonate nodules are occasionally phosphatized along grain contacts, but for the most part are still calcite. Detailed examination of these is beyond the scope of this investigation, and when the term "nodule" is used in this report, it refers only to the phosphorite nodules.

Peloids are subspheroidal and are composed of collophane (cryptocrystalline apatite). They are generally on the order of 100 to 150 microns in long dimension, but can range up to 300 microns long. The peloids exhibit a wide range of abundance from nodule to nodule, with some nodules being dominated by peloids, others consisting chiefly of radiolarians, and many nodules containing high percentages of both grain types. Some of the peloids contain faint ghosts of radiolarian tests.

Robbins and Porter (1980) contended that fecal pellets (perhaps excreted by zooplankton, e.g. copepods) are the main supplier of phosphorus to the sediment in various phosphatic shales (including the mid-continent Pennsylvanian Excello Shale). Many of the peloids in the present study could be fecal in origin as they are comparable in size and shape to those described by Robbins and Porter (1980), but a number of the peloids appear to have been produced diagenetically through

degradation of radiolarians. Soudry and Nathan (1980) illustrated a wide variety of diagenetic mechanisms that can create phosphatic peloids, including alteration of microfossil tests.

Whether the origin of the peloids is fecal, diagenetic, or both requires further study, but these peloids are often rimmed with apatite cement, indicating that they acted as nucleation sites for apatite precipitation, and suggesting that the peloids may have supplied phosphorus to the sediment.

Cements

Apatite and calcite constitute the dominant cements in the phosphorite nodules. Silica is locally important as a cement, and in some places replaces fossil fragments. Pyrite is also present in many nodules.

Apatite cement usually occurs as a thin (up to 25 microns thick), radiating, isopachous rind nucleating around various grain types including radiolarian tests, peloids, clumps of organic spheroids, and large skeletal grains (Figure 16). The degree of cementation by apatite within any given nodule is variable. Some nodules display distinct, well-defined rims of apatite cement whereas others display more pervasive cementation. In this latter case, the rims of cement are not well-defined, and they exhibit evidence of compaction. In a few cases faint evidence of dissolution is visible on apatite rims.

Calcite cement commonly occurs in the nodules as large (up to three mm in diameter) irregular crystals that are occasionally clear, but are more often somewhat spotted (with pyrite in many cases). Void

Figure 16. Photomicrographs of apatite cement.

a. Radiolarian encased in apatite cement. Note apatite rims around individual radiolarian spines. Nodule is from Tacket Shale at locality OHC. Bar scale = 75 microns. Plane polarized light.

b. Radiolarian encased in apatite cement. Note apatite rim around outer portion of test (arrow). Nodule is from Stark Shale at locality DSW. Bar scale = 40 microns. Plane polarized light.

c. Rim of apatite cement nucleated on a radiolarian spicule. Clear cement in background is silica. Nodule is from Tacket Shale at locality K-57. Bar scale = 40 microns. Plane polarized light.

d. Radiating, botryoidal apatite cement. Clear cement is silica. Nodule is from Tacket Shale at locality K-57. Bar scale = 15 microns. Plane polarized light.

Figure 16

A

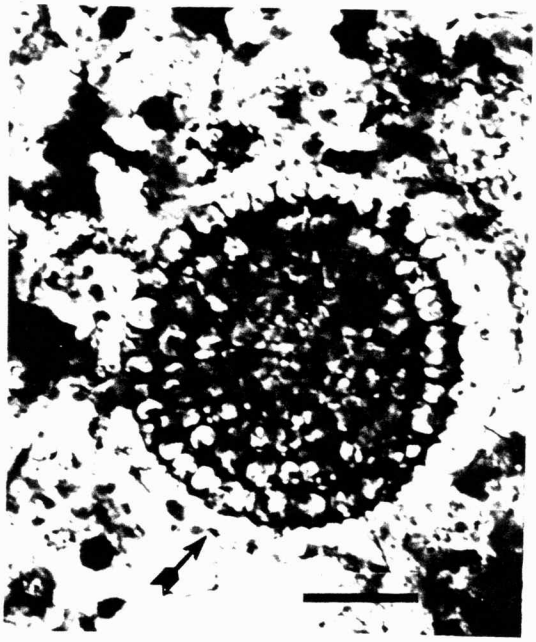

B

C

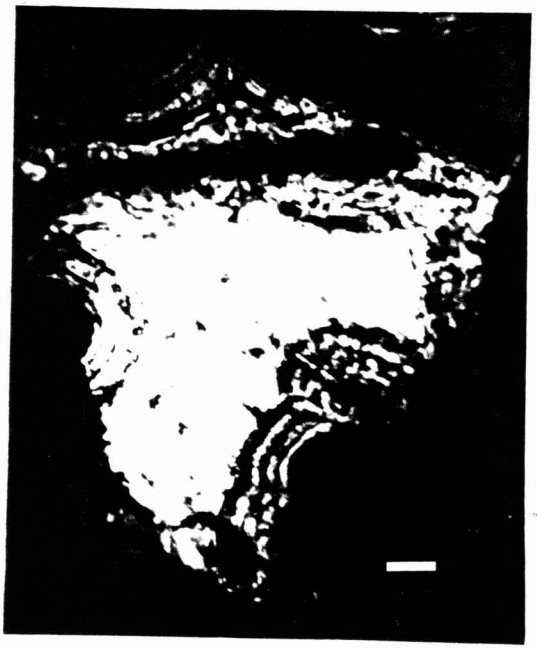

D

space in the few megafossils preserved in the nodules is filled with large calcite crystals (Figure 17a, b), and calcite also occurs as intergranular cement.

Silica is absent or rare in many nodules, but finely crystalline silica cement and chalcedony are commonly observed in some nodules (Figure 17b, c). The source of silica is undoubtedly radiolarians probably supplemented by sponges. Some silica occurs as a replacement of skeletal grains (Figure 17b).

Pyrite occurs as a replacement mineral in numerous phosphorite nodules. Usually it occurs as finely disseminated crystals throughout a given nodule, although sometimes it selectively replaces skeletal grains, and on rare occasions, it replaces the better part of an entire nodule (Figure 17d). In many cases the pyrite seems to preferentially replace calcium carbonate.

Laminae

Petrographic examination of laminae reveals that they consist of discontinuous layers that are composed of tiny "micronodules" (Figure 15c). These "micronodules" resemble larger phosphorite nodules in that they display the same types of relationships with the surrounding shale, and they are occasionally cemented by calcite and rarely silica. Laminae differ from nodules in that the phosphorite composing them is entirely collophane. No radiating, isopachous cement is preserved. Questionable organic spheroids are the only distinguishable remains of life preserved in the laminae.

Figure 17. Photomicrographs of cements.

a. Large calcite crystals within nautiloid chambers. Arrow denotes siphuncle. Nodule is from Anna Shale at locality Els. Bar scale = 1.3 mm. Doubly polarized light.

b. Unidentified shell containing calcite cement. The shell has been replaced by finely crystalline silica (arrow). Nodule is from Muncie Creek Shale at locality Ktl. Bar scale = 500 microns. Doubly polarized light.

c. Chalcedony in a nodule from Tacket Shale at locality K-57. Bar scale = 75 microns. Doubly polarized light.

d. Partial replacement of a calcite vein by pyrite. Nodule is from Anna Shale at locality Els. Most of this nodule has been pyritized Bar scale = 180 microns. Plane polarized light.

Figure 17

A

B

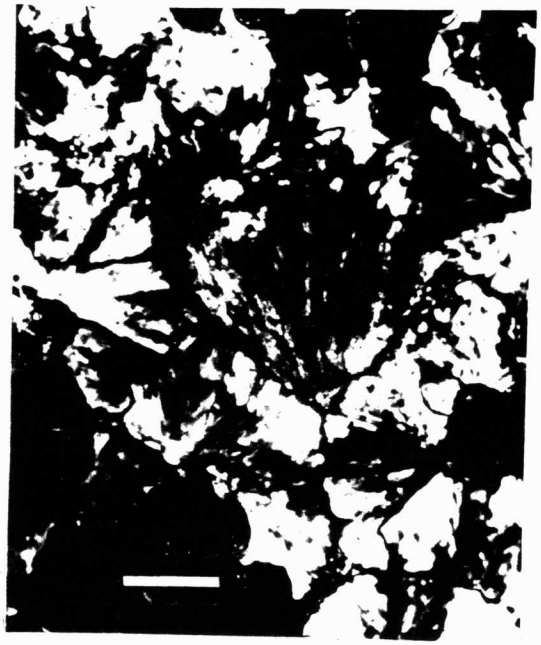

C

D

PALEONTOLOGY

Microfossils

Radiolarians (first reported by Berendsen and Nodine-Zeller, 1978) are the dominant skeletal grain type found in mid-continent Pennsylvanian phosphorite nodules. This biota consists of spumellarians that display tests with varying numbers, types, and lengths of spines, as well as a variety of pore arrangements, indicating a diverse fauna as verified by Nodine-Zeller et al. (1979). This mid-continent fauna represents the first well-preserved Pennsylvanian radiolarians reported from North America (Nodine-Zeller et al., 1979), and the assemblages are currently under study by B.K. Holdsworth. Nearly all of the radiolarians have been phosphatized, although some retain a partially siliceous test.

Preservation ranges from exquisite to poor, and various stages of degradation of radiolarians can often be examined within a single nodule. Apatite cement commonly nucleates around the skeleton, as well as around individual spines and spicules (Figure 16 and 18a). One outstanding example preserves the outer wall of the radiolarian, from which a rind of apatite has grown inward toward the phosphatized skeleton. Furthermore, what appears to have been the protoplasm of the organism has been splendidly preserved by phosphate (Figure 18b).

These radiolarians clearly provided nucleation sites for the precipitation of apatite cement, and phytoplankton possibly

Figure 18. Photomicrographs of Radiolaria.

a. Radiolarian from Tacket Shale at locality K-57. Note rims of apatite cement around spines. Bar scale = 35 microns. Plane polarized light.

b. Radiolarian from Tacket Shale at locality K-57. Note internal skeleton preserved within what may be phosphatized remnant of protoplasm. Also note (arrow) rind of cement that precipitated inward from what was either an outer portion of radiolarian skeleton or perhaps outer protoplasm wall. Bar scale = 50 microns. Plane polarized light.

c. Delicately preserved radiolarian from Stark Shale at locality DSW. Bar scale = 30 microns. Plane polarized light.

d. Radiolarian from Anna Shale at locality OCBE. Bar scale = 40 microns. Plane polarized light.

Figure 18

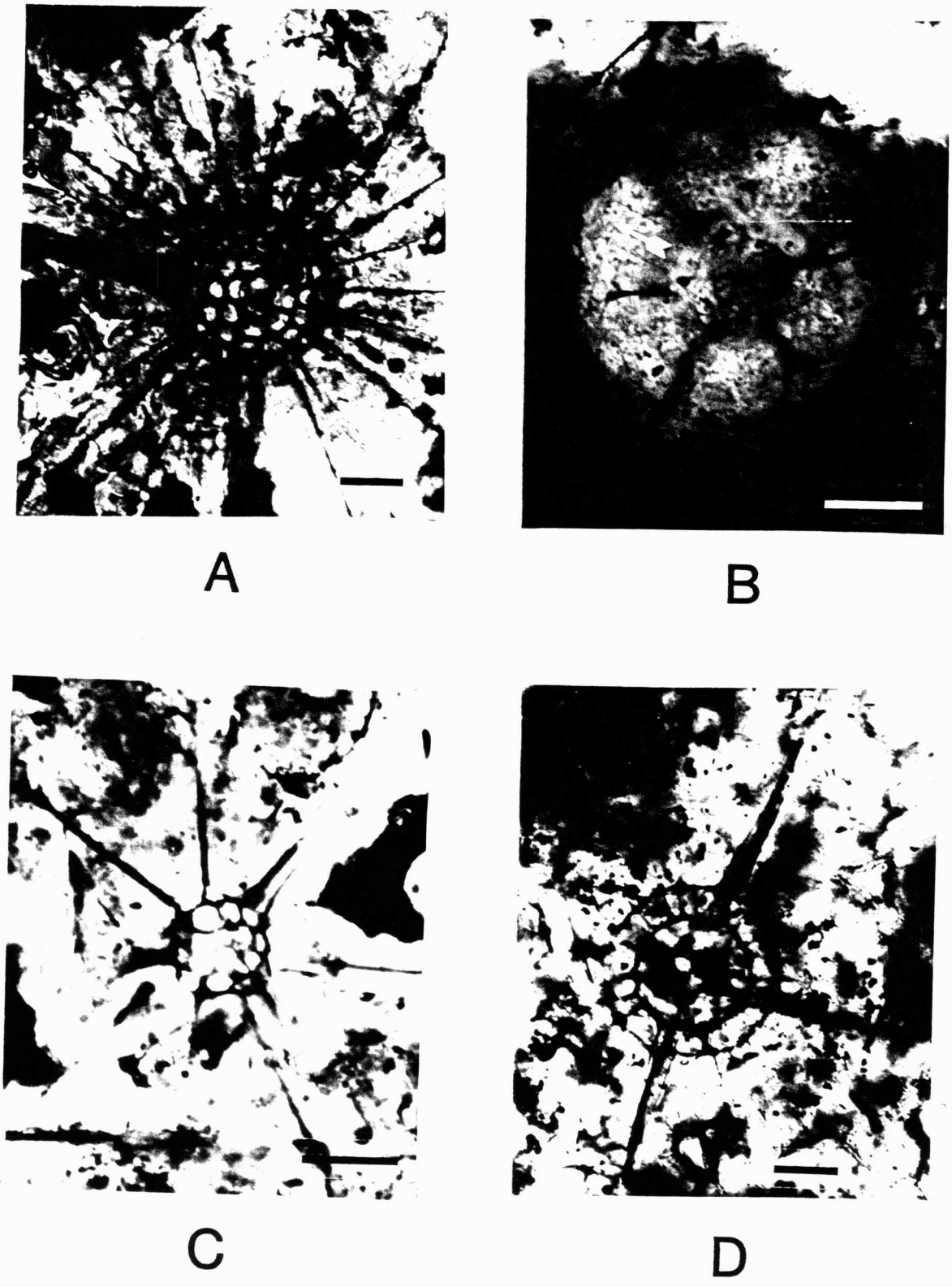

supplemented by the radiolarians probably supplied much phosphorus to the sediment.

Thirty-one shales from the study area were processed for palynomorphs with little success. Only four of the shales yielded palynomorphs of any sort, and those found were exceedingly rare. The most diagnostic of these palynomorphs probably belong to the Tasmanaceae, whose living counterparts are cysts affiliated with planktonic green algae (Williams, 1978; Brasier, 1980). The specimens are not abundant, and only moderately well-preserved. They range from 40 to 60 microns in diameter, and show very little variation in sculpturing (Figure 19a).

Unadorned organic-walled spheroids are preserved in shale macerals, but are much more common in thin sections of the nodules. The spheroids are dark brown and rarely exceed 10 microns in diameter. These are probably algal, and some could represent zooxanthellae (symbiotic cells) associated with the radiolarians as is the case in modern radiolarians (Kling, 1978). Apatite cement occasionally nucleates around small clusters of these spheroids.

Sponge spicules (Figure 19c; also previously reported by Berendsen and Nodine-Zeller, 1978) and poorly preserved fragments of tiny (algal?) tubes were the only other types of microfossils observed in the nodules.

Megafossils

Nautiloids (Figure 19b), bone fragments (fish?), inarticulate brachiopods, and vascular plant material (Figure 19d) constitute the

Figure 19. Photomicrographs of selected biota.

a. Palynomorph of family Tasmanaceae. Specimen recovered from a maceral of black shale (Tacket) at locality OHC. Bar scale = 8 microns. Plane polarized light.

b. Nautiloid from Anna Shale at locality Els. Chambers are filled with calcite cement. Portions of shell and some areas of cement have been pyritized (arrow). Bar scale = 1.2 mm. Plane polarized light.

c. Sponge spicules from Anna Shale at locality JQ. Bar scale = 40 microns. Plane polarized light.

d. Phosphatized vascular plant material from Anna Shale at locality Els. Light colored background is calcite cement. Bar scale = 2 mm. Plane polarized light.

Figure 19

A

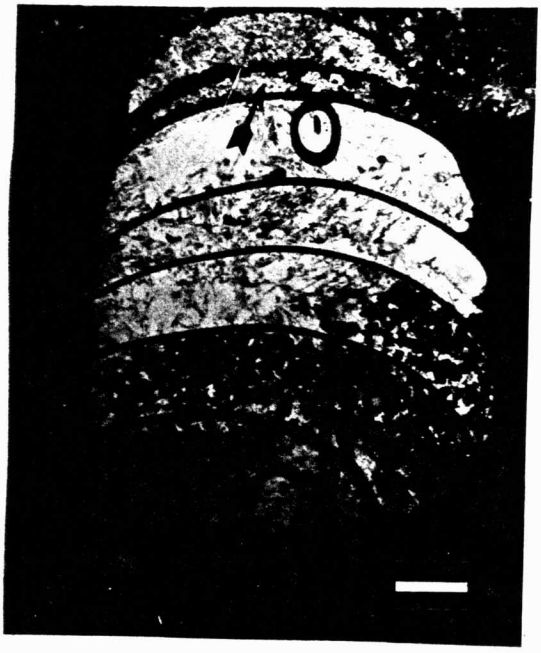

B

C

D

identifiable megafossils found in these nodules. Other organisms (e.g. trilobites, R. K. Pabian, pers. comm.) have been reported in mid-continent Pennsylvanian nodules, but megafossils are not central to this study, and it suffices merely to mention and briefly illustrate the types present.

DIAGENESIS

Diagenetic relationships within the phosphorite nodules are often difficult to assess, as the nature of the contacts between different types of cements is often vague, and few nodules contain all of the cements discussed earlier. By examining a number of nodules that display well-defined contacts between cements, an overall diagenetic sequence for the nodules can be inferred (Figure 20).

Apatite cement precipitated first, principally as thin, isopachous, radiating rims on many grain types. These rims represent the earliest stage of void-filling within the nodules and occur around the outer portions of intragranular and intergranular voids. In a few places it appears that the apatite rims have experienced a slight degree of dissolution.

Silicification and calcitization constitute the next stages of cementation within the nodules. Only in rare cases does one find both silica and calcite within a single nodule, and the two cements have not been observed in physical contact, making it difficult to interpret the timing of the two events. Both cements occur within voids that are rimmed with apatite cement. Where little or no silica or calcite is present, grains within the nodules are often compacted slightly.

Figure 20. Generalized diagenetic sequence in mid-continent Pennsylvanian phosphorite nodules. R = radiolarian, P = peloid.

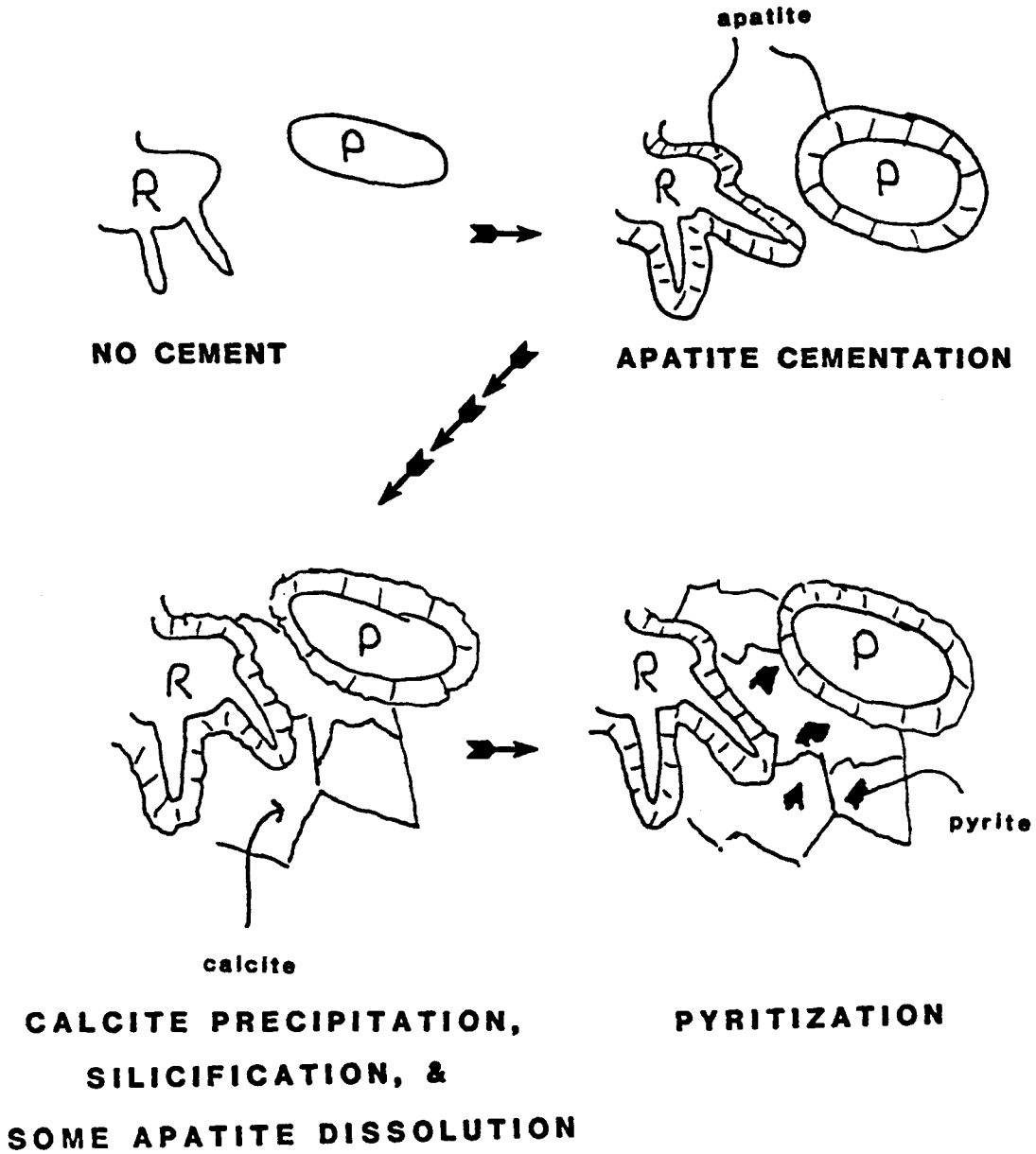

All of the above cements are interpreted as void-filling largely because they occur in intergranular and intragranular voids. The apatite rim cements, large calcite crystals, and chalcedony all appear void-filling in origin. Some of the finely crystalline silica is replacive as seen in the unidentified shell fragment in Figure 17b. This replacive silica is virtually identical to much of the other finely crystalline silica in the nodules. However, at least some of the finely crystalline silica cement may be void-filling where it grades into the few examples of chalcedony.

Pyrite represents the final stage of mineralization within the nodules. It replaces phosphate (usually collophane), calcite, and silica, but most often replaces calcite.

ORIGIN OF MARINE PHOSPHORITES

The last decade has produced a wealth of information concerning the origin of marine phosphorites. Cook (1976) and Bentor (1980) provide excellent summaries of recent progress made in phosphorite research.

Phosphorites on the sea floor today are situated on pericontinental shelves. They have been deposited at depths of 60 to 450 meters in areas of slow clastic influx, upwelling, and high organic productivity at low paleolatitudes. A possible sequence of events leading to the formation of marine phosphorites has been synthesized by Bentor (1980). In this sequence, upwelling currents driven by prevailing winds supply the nutrients necessary to support high pelagic productivity. Upon death, the organisms sink to the bottom, releasing the phosphorus in their systems to the sediment as they decay. This improves the chances for apatite formation by either replacement of calcium carbonate or by direct precipitation of apatite beneath the sediment/water interface.

Much of this theory had been derived from earlier studies based on phosphorites deposited in west-coast upwelling areas. In 1970, Kolodny and Kaplan dated many of these deposits using uranium-series disequilibrium methods, and found that all of the phosphorites in their study were older than 700,000 years, apparently leaving us

with no direct modern analog for phosphorite formation. Three Holocene examples have subsequently been found: on the Namibian shelf (Baturin et al., 1972), the Peru/Chile shelf (Burnett and Veeh, 1977), and the East Australian continental margin (Kress and Veeh, 1980; O'Brien and Veeh, 1980). The first two of these are situated on west coasts, where upwelling causes high productivity. The third however, occurs in an area of only moderate seasonal upwelling, and fairly low organic productivity.

It is probable that planktonic microorganisms are an important factor in supplying phosphorus to these sediments. Trudinger (1979) calculated that phytoplankton in upwelling environments could supply all the phosphorus necessary to form "a major phosphorite deposit in a geologically reasonable time." This function is apparently fulfilled by diatoms (Baturin, 1970; Burnett, 1977) and dinoflagellates in the Holocene west-coast deposits, and by bacteria in the East Australian deposits (O'Brien and Veeh, 1981). Fecal pellets also probably contribute significantly in supplying phosphorus to the sediment (Robbins and Porter, 1980).

Modern phosphorites are believed to form beneath the sediment/water interface. Firstly, although the results of some experimental work done by various workers on the solubility of apatite remain in conflict (Roberson, 1966; Atlas, 1979), it remains a strong possibility that seawater may be undersaturated with respect to phosphorus. Furthermore, phosphorus concentrations are commonly one to two orders of magnitude higher in interstitial waters within

anoxic sediments (Bentor, 1980). Secondly, Martens and Harriss (1970) have shown that magnesium inhibits the precipitation of apatite, making it very unlikely that apatite precipitates directly from seawater. Diagenetic formation of minerals in the sediment that contain magnesium (e.g. clays) could decrease or remove the effects of Mg-inhibition.

Birch (1980) reported an example of a lagoonal phosphorite (some of it primary) in an area of extremely low detrital influx on the western margin of southern Africa. This probably does not apply to these Pennsylvanian phosphorites, as demonstrably nearshore environments in the mid-continent Pennsylvanian are generally subject to significant amounts of clastic influx. The lateral continuity of the black to gray shales that enclose these Pennsylvanian phosphorites also precludes a lagoonal origin.

The Permian Phosphoria formation of the western United States is perhaps the most thoroughly studied ancient phosphorite deposit (McKelvey et al., 1953), and it represents an ancient example of the modern pericontinental west-coast upwelling type of deposit. Jacobsen et al. (1982) recently reported the occurrence of acritarchs (problematic marine algal cysts; Downie, 1973) in phosphorite layers, but not in the interbedded mudstones. This suggests that phytoplankton may have been important in the genesis of the Permian phosphorite layers in the Phosphoria.

Cook and McElhinny (1979) reviewed the history of phosphorite deposition within the framework of plate tectonics. Their model

suggests that major phosphogenic provinces can be generated only when the continents are in the proper position to allow for upwelling in low latitudes. Their study provides a working hypothesis for explaining the distribution of phosphorites spatially and temporally. The plate tectonics model does not incorporate phosphorites deposited in epicontinental seas, perhaps due to limited information concerning phosphorites in either modern or ancient epicontinental seas.

DEPOSITIONAL ENVIRONMENT OF THE PENNSYLVANIAN BLACK SHALES

Black shales can be formed in a wide variety of sedimentary environments, ranging from shallow lagoons to abyssal depths. All of these situations cannot be discussed here, but it is important to briefly review the controversies involving the deposition of these mid-continent Pennsylvanian black shales.

The three major depositional regimes that have been proposed to explain the depositional environment of the Pennsylvanian mid-continent black shales include: 1) shallow shoreline environments, 2) a silled basin, and 3) deposition in an offshore environment below a thermocline.

Moore (1929) proposed a nearshore swamp environment for the black shales. Zangerl and Richardson (1963) and Merrill (1975) expanded on the swamp idea by invoking a flotant of seaweed to generate anoxic conditions necessary for black shale deposition.

Two types of sills have been proposed to create anoxic conditions in the mid-continent Pennsylvanian. Evans (1966) suggested that detrital sedimentation near the mouth of the basin may have restricted circulation enough to produce anoxic conditions. Wilson (1975) illustrated a situation in which black shales may have accumulated adjacent to sills created by organic banks.

A recent model (Heckel, 1977) placed the black shale in an offshore position in an epicontinental sea in which water became deep enough to develop anoxic conditions below a thermocline. This model also called for deposition of phosphorite as a result of wind driven quasi-estuarine circulation (upwelling) that promoted the development of a circulatory nutrient trap (Brongersma-Sanders, 1971) which progressively increased the amount of organic matter in the system. As organic matter sank to the bottom, it decayed, enhancing anoxic conditions on the bottom and releasing its phosphorus into the sediment.

Heckel's model deals most directly with the widespread, laterally continuous shales of this study, and it best explains the origin of the phosphorite. Furthermore, two types of black shales have now been recognized (Heckel, 1977; Heckel and Swade, 1977; Merrill and von Bitter, 1976) in the mid-continent Pennsylvanian, namely: 1) discontinuous black shales that grade into nearshore deposits, contain sandy layers, and lack non-skeletal phosphorite, and 2) laterally continuous black shales that grade only into gray shales with high faunal diversity, indicating open marine conditions. Only these latter shales contain abundant non-skeletal phosphorite.

Discontinuous black shales from the Cherokee Group (Middle Pennsylvanian) of Iowa have yielded only terrestrial palynomorphs (J. Utting, pers. comm., 1981). The laterally continuous shales in the present study yielded only occasional tasmanitid palynomorphs. Price (1981) reported that palynomorph abundance decreases

progressively upward from terrestrial shales toward the black shale while maintaining good preservation throughout. This distribution of palynomorphs strongly supports deposition of these black shales in an offshore regime.

The coastal swamp model may explain the discontinuous nonphosphatic black shales, and the silled basin model could account for more widespread black shales, but only the offshore upwelling model accounts for both the non-skeletal phosphorite and widespread nature of the mid-continent black shales.

DEPOSITIONAL MODEL FOR PENNSYLVANIAN PHOSPHORITES OF THE MID-CONTINENT

The petrology of these Pennsylvanian epicontinental sea phosphorites suggests that they were deposited under conditions similar to those of Holocene pericontinental sea phosphorites. The west-coast Holocene examples develop in areas of upwelling and high pelagic productivity, with phosphate replacing calcareous microfossils (Manheim et al., 1975) and precipitating directly on diatoms below the sediment/water interface (Baturin, 1970; Burnett, 1977). Bacteria supply phosphorus to the sediment in the absence of other pelagic organisms on the east coast of Australia (O'Brien et al., 1981). Plankton and fecal material (supplemented to some degree by other pelagic organisms) probably supplied phosphorus to the sediment in these Pennsylvanian phosphorites.

Conditions favorable to the precipitation of apatite are very similar to those favoring calcite precipitation (Bentor, 1980; Krauskopf, 1979). Seawater usually contains a much greater proportion of the components necessary to form calcium carbonate so that if any apatite were precipitating at the same time as calcite, it would be completely overwhelmed by calcium carbonate. Calcium carbonate is generally unstable at a pH lower than 7.5, while apatite remains stable down to a pH of 7.0 (Bentor, 1980).

Ames (1959) demonstrated that it is much easier to form phosphorites by the replacement of calcium carbonate than to precipitate apatite directly. Many phosphorites form as a result of replacement of calcium carbonate, but the phosphorites of this study formed largely by primary apatite precipitation, most likely below the sediment/water interface. The occasional carbonate nodules found in the gray (and sometimes black) shales have only been slightly phosphatized, and phosphorite nodules in the black shales are lacking in skeletal carbonate.

A likely sequence of events leading to the development of the Pennsylvanian epicontinental sea phosphorites begins with the establishment of quasi-estuarine circulation leading to the development of a circulatory nutrient trap (Brongersma-Sanders, 1971) as modified by Heckel (1977) for these deposits (Figure 21). Plankton, fecal pellets, and pelagic megafossils sank to the bottom after death where they began to decay, releasing phosphorus to the sediment. The organic decay may have lowered the pH of the interstitial waters creating conditions that would allow for the precipitation of apatite below the sediment/water interface while inhibiting the precipitation of calcite. Development of apatite cement could then have arrested the organic degradation allowing for exquisite preservation of radiolarians. As organic decay diminished, the pH of the interstitial waters may have risen enough to allow for calcite precipitation in many nodules. Alternatively, most of the dissolved phosphorus may have been used up during apatite cementation,

Figure 21. Depositional model for formation of mid-continent Pennsylvanian phosphorites. Modified from Brongersma-Sanders (1971) and Heckel (1977).

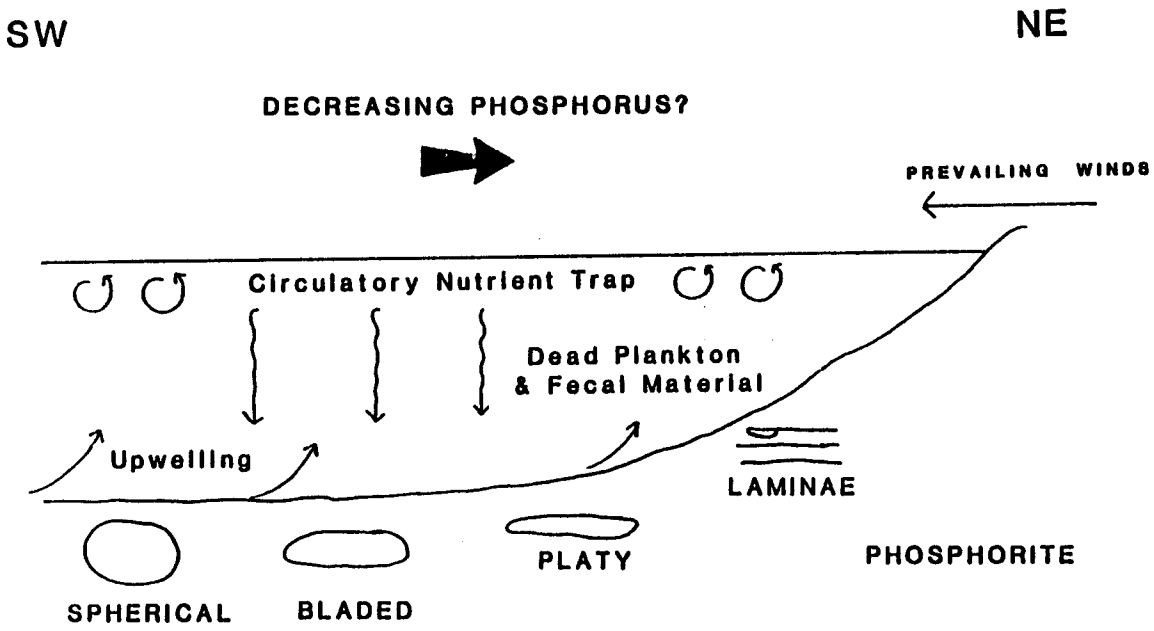

which then was followed by calcite and silica cementation.

Nodules seem to be largest in the upper and lower portions of the black shales (near the contact between the gray and black facies). This could bear a close relationship to the occurrence of most modern phosphorite at the upper and lower boundaries of the oxygen minimum zone off the coast of Peru (Burnett and Veeh, 1977; Burnett et al., 1980; Burnett et al., 1982).

The close resemblance between the general set of conditions under which modern pericontinental and these Pennsylvanian epicontinental sea phosphorites form suggests a close genetic relationship between the two analogs. The modern phosphorites off the coast of Peru have been shown (Burnett et al., 1982) to form very slowly, at rates on the order of a few millimeters per thousand years. Considering the close similarities between modern and Pennsylvanian phosphorites, it seems difficult to believe that any of these widespread Pennsylvanian black shales could have been deposited in as short a period of time as four years as had been previously proposed (Zangerl and Richardson, 1963).

The decrease in nodule thickness with increasing distance from the outlet to the epicontinental sea may represent decreasing significance of one or several of the conditions that facilitated phosphorite formation. Some of these factors could be: 1) a decrease in the amount of phosphorus available, perhaps as many of the nutrients were taken up by the biota in the southern portions of the sea; 2) decreased or less regular occurrence of upwelling

farther from the outlet; 3) variations in sedimentation rate, with phosphorites being more conspicuous during periods of slower sedimentation due to decreased sediment dilution.

SUMMARY

Widespread mid-continent Pennsylvanian black shales are characterized by nodular to laminar phosphorites. The nodules vary laterally in shape, grading from spherical in Oklahoma and southern Kansas to progressively more bladed and platy forms in northeastern Kansas. Nodule size varies locally with large nodules predominating in thicker shales and small nodules dominating thinner shales. Nodules decrease in size from northern Kansas into Missouri where they often grade laterally into phosphorite laminae. In Iowa, non-skeletal phosphorite is observed only as laminae.

Petrographic investigation reveals abundant and diverse radiolarians preserved in the phosphorite nodules. Many nodules consist of a framework of phosphatized radiolarian tests that served as nucleation points for apatite cement. Peloids also contribute to the phosphorite nodules, and pelagic megafossils (e.g. nautiloids and fish bones) occasionally are included in the nodules. Detrital material that might suggest proximity to terrestrial influence is notably absent in the phosphorites.

These phosphorites are interpreted as having formed through the following sequence of events:

1) Establishment of quasi-estuarine circulation.

2) Development of a prolific pelagic biota in a circulatory nutrient trap.

3) Release of phosphorus to the sediment by decaying organic matter (mainly plankton and fecal material).

4) Cementation by apatite followed by calcitization and silicification.

5) Pyritization.

The occurrence of many of these mid-continent Pennsylvanian phosphorites near the boundary between gray and black shale, and the predominance of larger nodules near the gray/black boundary in those shales in which phosphorite is distributed throughout, may relate closely to the fact that modern Peruvian phosphorites largely occur near the upper and lower boundaries of the oxygen minimum zone.

CONCLUSIONS

The results of this study suggest the following conclusions:

1) These phosphorites formed primarily by direct precipitation of apatite below the sediment/water interface, not as a replacement of calcium carbonate.

2) These epicontinental sea phosphorites probably formed in a similar fashion to Holocene pericontinental phosphorites, and they formed very slowly, on the order of a few millimeters of growth per thousand years.

3) The probable mode of formation of these phosphorites combined with the lack of terrigenous detrital material and the widespread nature of the enclosing shales limits the depositional environment of the widespread Pennsylvanian black shales to an offshore, sediment-starved regime.

REFERENCES

Ames, L.L., 1959, The genesis of carbonate-apatite: Econ. Geol., v. 54, p. 829-841.

Atlas, E.L., 1979, Solubility controls of carbonate-fluorapatite in seawater: Rep. on the Marine Phosphatic Sediments Workshop, Honolulu, 1979, W.C. Burnett and R.P. Sheldon (eds.), p. 18-20.

Baturin, G.N., Kochenov, A.V., and Petelin, V.P., 1970, Phosphorite formation on the shelf of S.W. Africa: Lith. and Min. Res., v. 3, p. 266-276.

Baturin, G.N., Merkulova, K.I., and Chalov, P.I., 1972, Radiometric evidence for recent formation of phosphatic nodules in marine shelf sediments: Marine Geol., v. 13, p. M37-M41.

Bentor, Y.K., 1980, Phosphorites - The unsolved problems: S.E.P.M. Sp. Pub., no. 29, p. 3-18.

Berendsen, P. and Nodine-Zeller, D.E., 1978, Radiolarian sponge-bearing phosphate nodules from Pennsylvanian black shales, southeastern Kansas: Geol. Soc. America, Abstr. w. prog., v. 10, p. 1-2.

Berner, R.A., 1980, Early diagenesis: A theoretical approach, Princeton University Press, 241 p.

Birch, G.F., 1980, A model of penecontemporaneous phosphatization by diagenetic and authigenic mechanisms from the western margin of southern Africa: S.E.P.M. Sp. Pub. no. 29, p. 79-100.

Brasier, M.D., 1980, Microfossils; George Allen & Unwin Ltd., London, 193 p.

Brongersma-Sanders, M., 1971, Origin of major cyclicity of evaporites and bituminous rocks; an actualistic model: Marine Geol., v. 11, p. 123-144.

Burnett, W.C., 1977, Geochemistry and origin of phosphorite deposits from off Peru and Chile: Geol. Soc. America Bull., v. 88, p. 813-823.

Burnett, W.C. and Veeh, H.H., 1977, Uranium-series disequilibrium studies in phosphorite nodules from the W. coast of S. America: Geochim. Cosmochim. Acta, v. 41, p. 755-764.

Burnett, W.C., Veeh, H.H., and Soutar, A., 1980, U-series, oceanographic, and sedimentary evidence in support of recent formation of phosphate nodules off Peru: S.E.P.M. Sp. Pub. no. 29, p. 61-71.

Burnett, W.C., Beers, M.J., and Roe, K.K., 1982, Growth rates of phosphate nodules from the continental margin off Peru: Science, v. 215, p. 1616-1617.

Cook, P.J. and McElhinny, M.W., 1979, A reevaluation of the spatial and temporal distribution of sedimentary phosphate deposits in the light of plate tectonics: Econ. Geol., v. 74, p. 315-330.

Crowell, J.C., 1978, Gondawanan glaciation, cyclothems, continental positioning, and climate change: Amer. Jour. Science, v. 278, p. 1345-1372.

Doher, L.I., 1980, Palynomorph preparation procedures currently used in the paleontology and stratigraphy laboratories, U.S. Geological Survey: U.S.G.S. circular 830, 29 p.

Downie, C., 1973, Observations on the nature of the acritarchs: Paleontology, v. 16, part. 2, p. 239-259.

Evans, J.K., 1966, Depositional environment of a Pennsylvanian black shale (Heebner) in Kansas and adjacent states (Unpub. Ph.D. thesis): Rice Univ., 162 p.

Heckel, P.H., 1977, Origin of phosphatic black shale facies in Pennsylvanian cyclothems of Mid-continent North America: A.A.P.G. Bull., v. 61, no. 7, p. 1045-1068.

Heckel, P.H., 1980, Paleogeography of eustatic model for deposition of midcontinent Upper Pennsylvanian cyclothems: Rocky Mtn. Sec. S.E.P.M., W-C. U.S. Paleogeog. Symp. 1, Paleozoic Paleogeography of west-central United States, T.D. Fouch and E.R. Magathan (eds.), p. 197-215.

Heckel, P.H. and Swade, J.W., 1977, Two types of Midcontinent Pennsylvanian black shales and their respective conodont faunas (abstr.): Geol. Soc. America, Abstr. w. Prog., v. 9, p. 604.

Jacobson, S.R., Wardlaw, B.R., and Saxton, J.D., 1982, Acritarchs from the Phosphoria and Park City formations (Permian, Northeastern Utah): Jour. Paleont., v. 56, no. 2, p. 449-458.

Kling, S.A., 1978, Radiolaria: in Introduction to Marine Micropaleontology, B.U. Haq and A. Boersma (eds.), Elsevier, New York, p. 203-244.

Kolodny, Y. and Kaplan, I.R., 1970, Uranium isotopes in sea floor phosphorites: Geochim. Cosmochim. Acta, v. 34, p. 3-24.

Krauskopf, K.B., 1979, Introduction to Geochemistry, McGraw-Hill, 617 p.

Kress, A.G. and Veeh, H.H., 1980, Geochemistry and radiometric ages of phosphatic nodules from the continental margin of northern New South Wales, Australia: Marine Geol., v. 36, p. 143-157.

Manheim, R.T., Rowe, G.T., and Jipa, D., 1975, Marine phosphate formation off Peru: Jour. Sed. Pet., v. 45, p. 243-251.

Martens, C.S. and Harriss, R.C., 1970, Inhibition of apatite precipitation in the marine environment by magnesium ions: Geochim. Cosmochim. Acta, v. 34, p. 621-625.

McKelvey, V.E., Swanson, R.W., and Sheldon, R.P., 1953, The Permian Phosphoria deposits of western United States: 19th Int. Geol. Congr. Algier, Section XI, p. 45-64.

Merrill, G.K., 1975, Pennsylvanian conodont biostratigraphy and paleoecology of northwestern Illinois: G.S.A. Microform Pub. 3.

Merrill, G.K. and von Bitter, P.H., 1976, Revision of conodont biofacies nomenclature and interpretations of environmental controls in Pennsylvanian rocks of eastern and central North America: Royal Ontario Mus. Life Sci. Contr. 108, 46 p.

Mitchell, J.C., 1981, Stratigraphy, petrography, and depositional environments of the Iola Limestone, Midcontinent U.S. (Unpub. Ph.D. thesis): Univ. of Iowa, 364 p.

Moore, G.E., 1979, Pennsylvanian paleogeography of the southern mid-continent: Tulsa Geol. Soc. Spec. Pub., no. 1, p. 2-12.

Moore, R.C., 1929, Environment of Pennsylvanian life in North America: A.A.P.G. Bull., v. 13, p. 459-487.

Moore, R.C., 1936, Stratigraphic classification of the Pennsylvanian rocks of Kansas: Kansas Geol. Surv. Bull. 22, 256 p.

Nodine-Zeller, D.E., Holdsworth, B.K., and Berendsen, P., 1979, Well-preserved Middle and Late Carboniferous radiolaria from Kansas, USA: (abstr.), Ninth Int. Congr. of Carboniferous Stratigraphy and Geology, p. 150.

O'Brien, G.W. and Veeh, H.H., 1980, Holocene phosphorite on the East Australian continental margin: Nature, v. 288, p. 690-692.

O'Brien, G.W., Harris, J.R., Milnes, A.R., and Veeh, H.H., 1981, Bacterial origin of East Australian continental margin phosphorites: Nature, v. 294, p. 442-444.

Price, R.C., 1981, Stratigraphy, petrography, and depositional environments of the Pawnee Limestone Middle Pennsylvanian (Desmoinesian), midcontinent North America (Unpub. Ph.D. thesis): Univ. of Iowa, 274 p.

Ravn, R.L., 1981, Stratigraphy, petrography, and depositional environments of the Hertha Limestone, Midcontinent U.S.A. (Unpub. Ph.D. thesis): Univ. of Iowa, 274 p.

Robbins, E.I. and Porter, K.G., 1980, Geologic importance of zooplankton fecal pellets in black shale associated with phosphate deposits: Palynology, v. 4, p. 249-250.

Roberson, C.E., 1966, Solubility implications of apatite in seawater: U.S.G.S. Prof. Pap. 550-D, p. D178-D185.

Runnels, R.T., Schleicher, J.A., and Van Nortwick, H.S., 1953, Composition of some uranium-bearing phosphate nodules from Kansas shales: Kansas Geol. Surv. Bull., 102, pt. 3, p. 93-104.

Schenk, P.E., 1967, Facies and phases of the Altamont Limestone and megacyclothem (Pennsylvanian), Iowa to Oklahoma: Geol. Soc. America Bull., v. 78, p. 1369-1384.

Sneed, E.D. and Folk, R.L., 1958, Pebbles in the Lower Colorado River, Texas, a study in particle morphogenesis: Jour. Geol., v. 66, p. 114-150.

Soudry, D. and Nathan, Y., 1980, Phosphate peloids from the Negev phosphorites: Geol. Soc. Lond. Jour., v. 137, pt. 6, p. 749-756.

Trudinger, P.A., 1979, Microbiological controls on phosphate accumulation: in P.J. Cook and J.H. Shergold (eds.), Proterozoic-Cambrian phosphorites, Canberra Publishing & Printing Co. Pty. Ltd., p. 87-92.

Wanless, H.R. and Shepard, F.P., 1936, Sea level and climatic changes related to Late Paleozoic cycles: Geol. Soc. America Bull., v. 47, p. 1177-1206.

Williams, G.L., 1978, Dinoflagellates, acritarchs, and tasminitids: in B.U. Haq and A. Boersma (eds.), Introduction to Marine Micropaleontology, Elsevier, New York, p. 293-326.

Wilson, J.L., 1975, Carbonate facies in geologic history, New York, Springer-Verlag, 471 p.

Zangerl, R. and Richardson, E.S., 1963, The paleoecological history of two Pennsylvanian black shales: Fieldiana-Geology Mem., v. 4, 352 p.

APPENDIX A

INDEX TO LOCALITIES

All localities are in Kansas unless otherwise stated.

Eudora Shale

Locality	County	Location
Copan (CpD)	Washington (OK)	T28N/R12E/S12/SE¼SE¼
Tyro Quarry (TyQ)	Montgomery	T34S/R15E/S30/SW¼SE¼
Pottawatomie Creek (PtC)	Anderson	T20S/R19E/S4/SW¼NW¼
Quarry East of Buffalo (NQEB)	Wilson	T27S/R16E/S23/NW¼NE¼
Kansas Rte. 10 (K-10)	Johnson	T12S/R21E/S36/SE¼SE¼

Muncie Creek Shale

Locality	County	Location
Canary Oil Field (Can)	Washington (OK)	T28N/R14E/S19/NE¼NW¼
Neodesha (Neo)	Wilson	T30S/R16E/S19/NE¼SW¼
Katy Lake (Ktl)	Allen	T24S/R20E/S13/SW¼NW¼
Kansas Rte. 32 (K-32)	Wyandotte	T11S/R25E/S7/SW¼SW¼

Stark Shale

Locality	County	Location
Dennis Southwest (DSW)	Labette	T31S/R18E/S21/SE¼NE¼
Type Stark (TSk)	Neosho	T27S/R20E/S14/SW¼SE¼
U.S. Rte. 169 (US-169)	Madison (IA)	T75N/R28W/S11/NE¼SW¼

Hushpuckney Shale

Locality	County	Location
Kansas Rte. 52 (K-52)	Linn	T22S/R23E/S23/NE¼SW¼
U.S. Rte. 69 (US-69)	Linn	T19S/R25E/S31/SE¼NW¼
Northwest of Prescott (NWP)	Linn	T22S/R24E/S24/SE¼SE¼
Iowa Pammel Park (IPP)	Madison (IA)	T75N/R28W/S16/SW¼
Iowa South of Winterset (ISW)	Madison (IA)	T75N/R27W/S6/S½

Lake Neosho Shale

Locality	County	Location
Oklahoma West of Hancock Bridge (OWHB)	Nowata (OK)	T27N/R16E/S10/SE¼SW¼
Keith Brother's Quarry (KBQ)	Labette	T34S/R17E/S35/SW¼NW¼
Neosho County State Lake (NCSL)	Neosho	T30S/R20E/S22/NE¼SE¼

Tacket Shale

Locality	County	Location
Oklahoma Hickory Creek (OHC)	Nowata (OK)	T28N/R15E/S14/NW¼NE¼
Wilsonton (Wltn)	Labette	T32S/R19E/S16/SW¼SW¼
Parsons Country Club (PCC)	Labette	T31S/R19E/S21/NE¼NE¼
Kansas Rte. 57 (K-57)	Neosho	T29S/R20E/S17/SE¼SE¼

"Dawson" Shale

Locality	County	Location
Oklahoma Double Creek (ODC)	Nowata (OK)	T25N/R15E/S27/SE¼SE¼
Mound Valley Southwest (MVSW)	Labette	T33S/R18E/S10/NE¼NE¼

Anna Shale

Locality	County	Location
Oklahoma Rte. 28 (O-28)	Nowata (OK)	T26N/R17E/S17/NW¼SE¼
Oklahoma Big Creek (OBC)	Craig (OK)	T29N/R18E/S27/NW¼NW¼
Oklahoma Coodies Bluff East (OCBE)	Nowata (OK)	T25N/R17E/S31/NW¼NW¼
Ellis School (Els)	Labette	T34S/R19E/S12/SW¼SW¼
Jubilee Quarry (JQ)	Bourbon	T26S/R24E/S16/SW¼SE¼

APPENDIX B

METHOD OF NODULE SHAPE CLASSIFICATION AND SHAPE DATA

This appendix describes the classification scheme used for comparison of nodule shapes. The classification is a modification of Sneed and Folk's (1958) form classification diagram.

The subdivisions of the triangular diagram are grouped into sections and subsections (Figure 22). Sections refer to major end members of the shape classification (Spherical-S, Bladed-B, Platy-P, and Elongated-E), and subsections refer to minor subdivisions such as SB or SP.

Measurements of the long, intermediate, and short axes of the nodules are plotted on the triangular diagram, and the percentage of nodules in each subsection is calculated (Figure 23). Percentages are then used to assign a letter designation for each nodule population as follows:

1) If the largest subsection (1) is greater than 50 per cent, the nodule population is named after the section to which the given subsection belongs, e.g. S, unless supplemented (see step 6).

2) If (1) is less than 50 per cent, but is greater than twice the size of the second largest subsection (2), and (2) is less than 20 per cent, the population is classified as X(Y) where X represents the dominant population, and Y represents a subordinate population.

Figure 22. Triangular diagram used for nodule shape classification (modified from Sneed and Folk, 1958). S = short axis, I = intermediate axis, L = long axis, V = very.

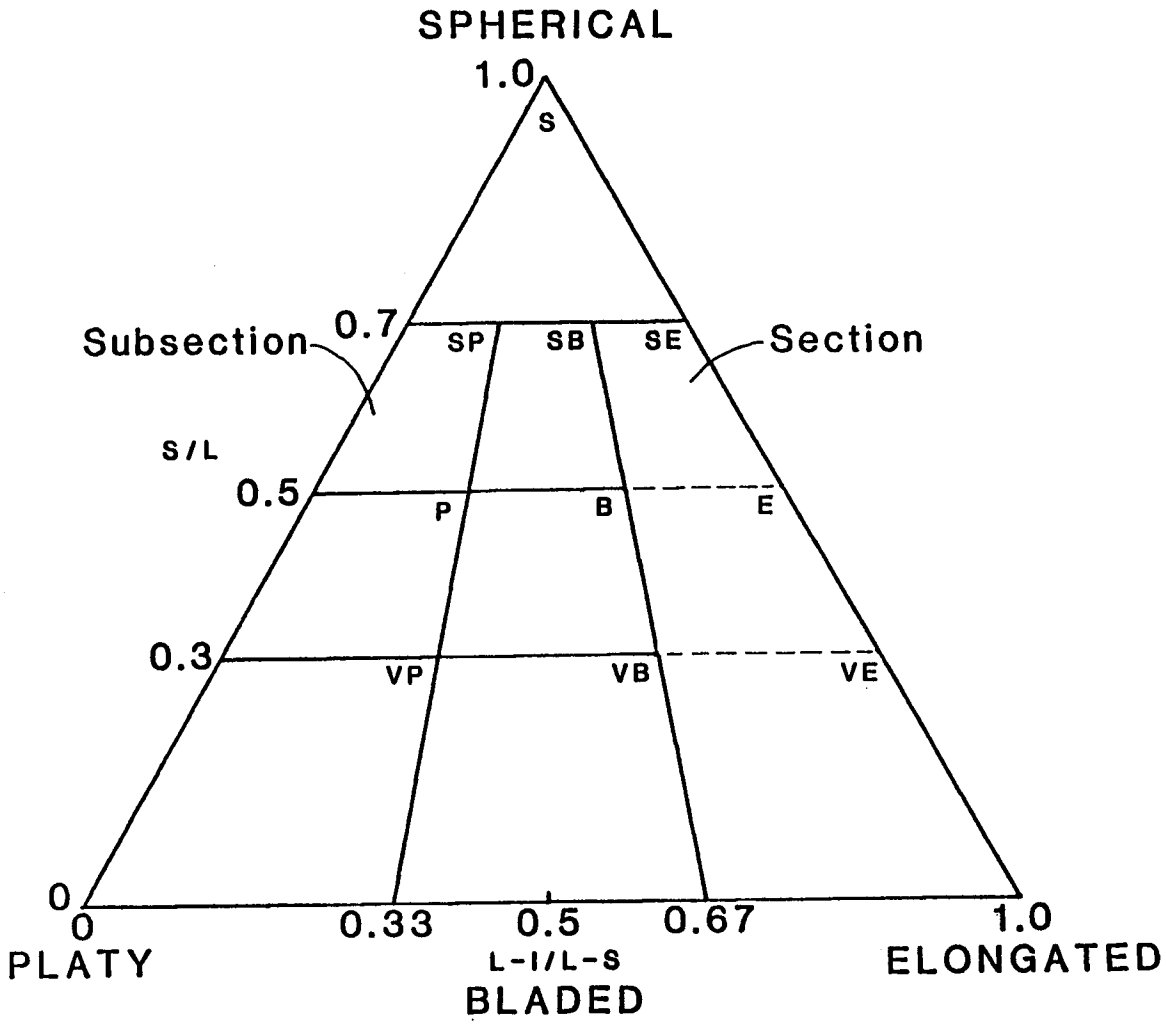

Figure 23. Sequence used in determining nodule shapes. Method outlined in Appendix B.

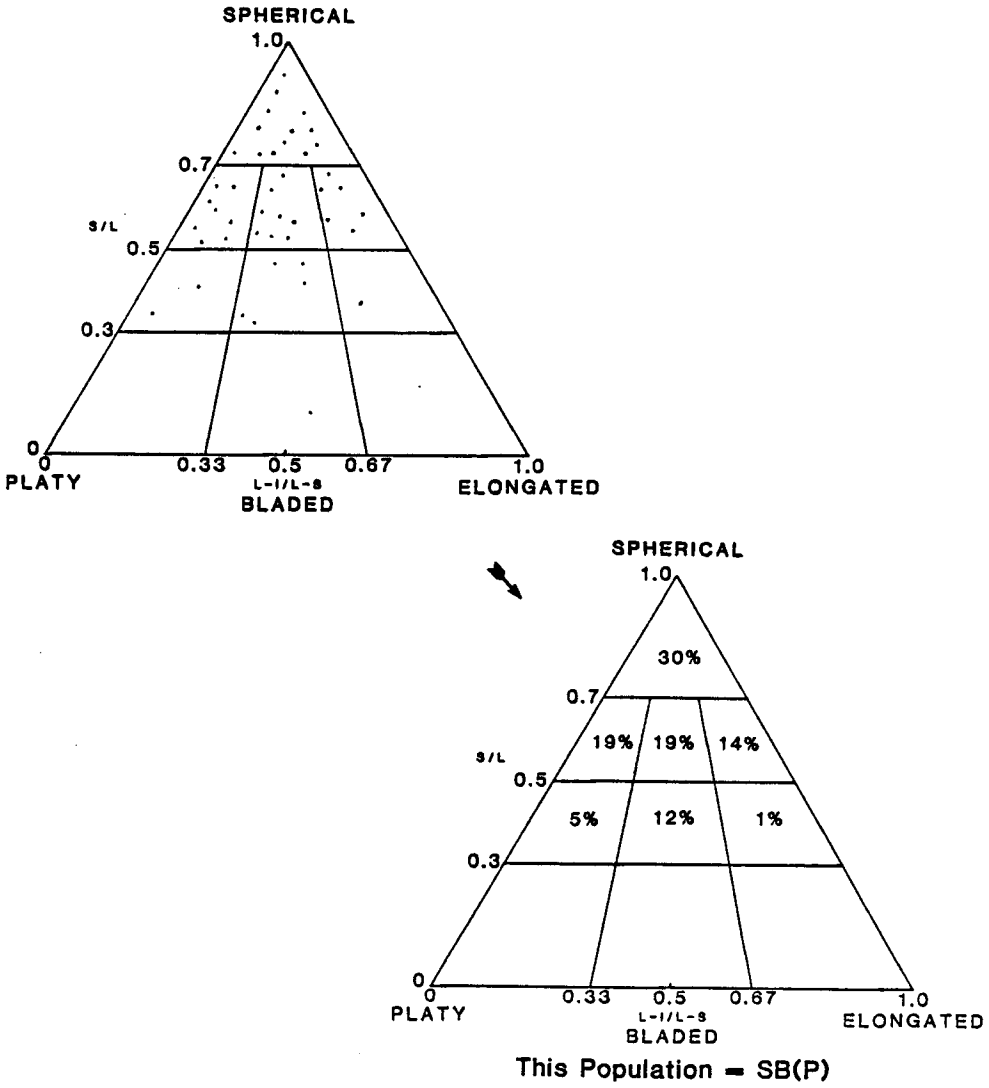

3) If the largest subsection (1) is less than twice the size (percentage) of the second largest subsection (2), the nodule population is named after both subsections with the larger subsection being listed first, e.g. SB.

4) If (1) = (2), and the third largest subsection (3) is greater than 15 per cent, (1) and (2) are listed, followed by (3) in parentheses, e.g. SB(P), unless (3) is in the same section as (1) or (2), in which case the dominant section is listed first regardless of which subsection is largest.

5) If (2) = (3), both (2) and (3) are listed in parentheses after (1), e.g. S(PB).

6) If (1) is greater than 50 per cent, but (2) is greater than 20 per cent or (2) = (3), and both (2) and (3) are in the same section, a supplemental shape factor is present. The supplement, (2), or (2) and (3) if (2) = (3), is listed in parentheses.

The shape axis used in Figures 9, 11, and 14 was derived in a semi-quantitative fashion by using a series of intermediates progressing from platy to spherical. Intermediates were plotted at equal increments along the shape axis in the order: P-PB-BP-B-BS-SB-S. Shape values were plotted at these points on the graph. Some shape values were intermediate between the values listed here and were plotted accordingly. The axis does not incorporate nodules with an SP shape, but this value was exceedingly rare for nodule populations studied here.

Figure 24. Shape data for Eudora Shale.

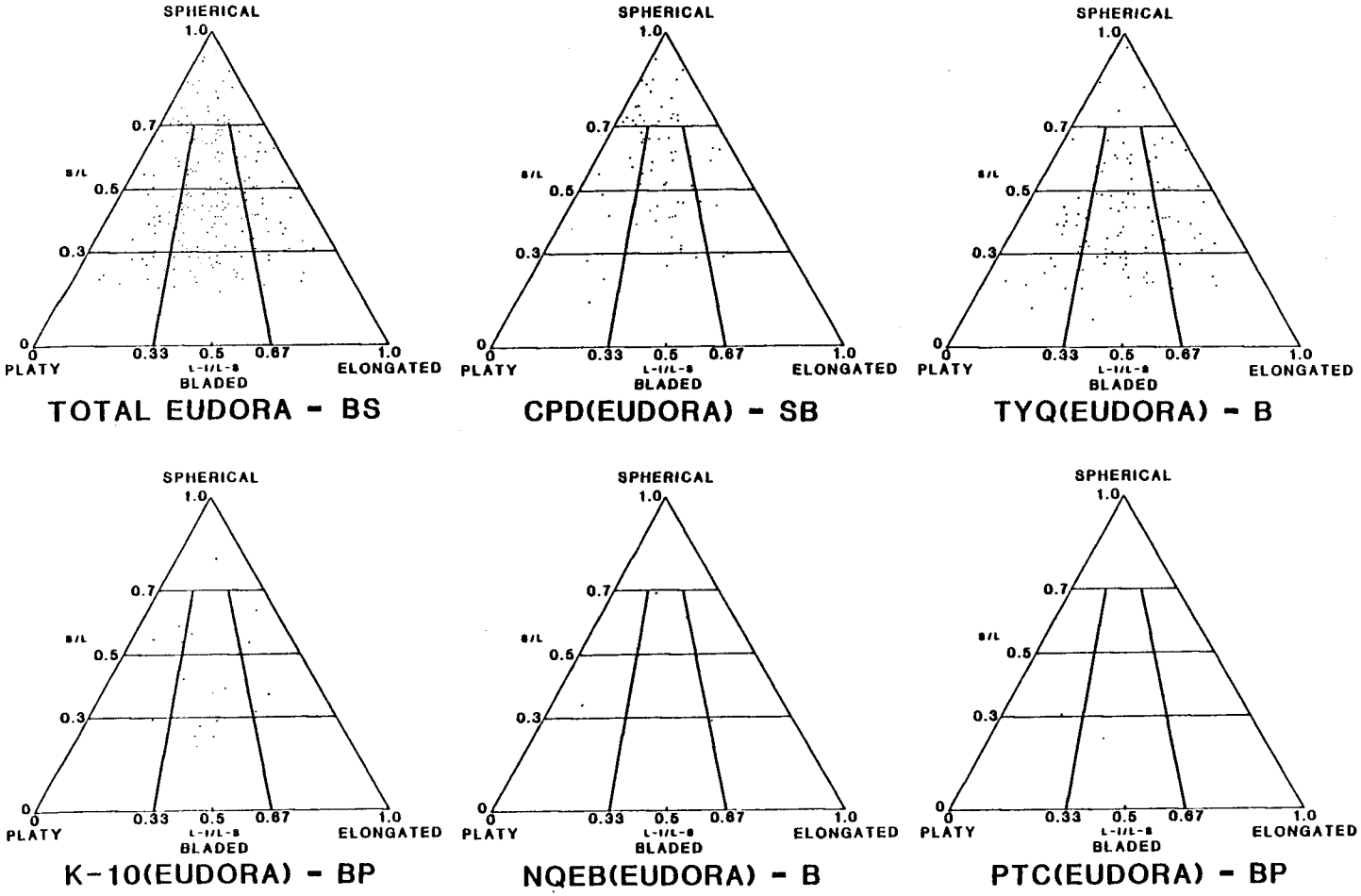

Figure 25. Shape data for Muncie Creek Shale.

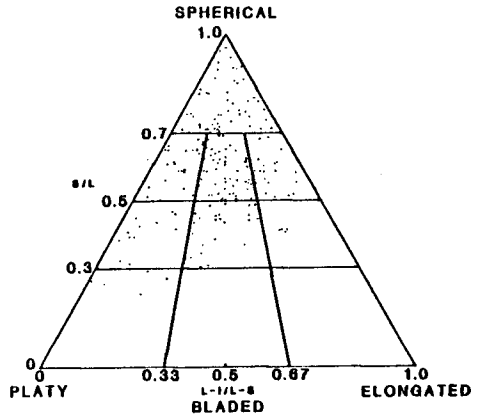

TOTAL MUNCIE CREEK - SB

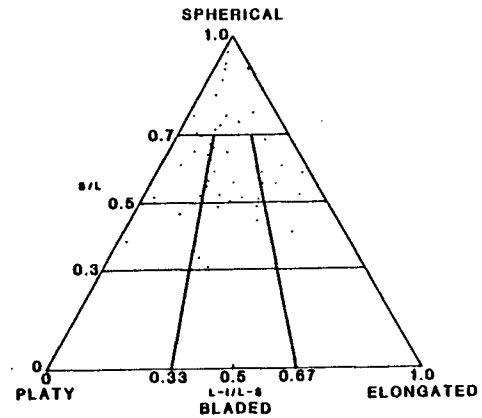

CAN(MUNCIE CREEK) - SB(P)

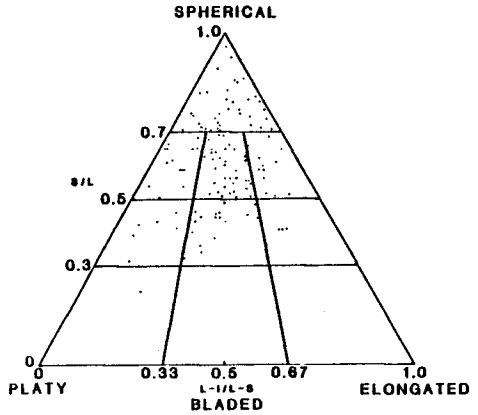

KTL(MUNCIE CREEK) - BS

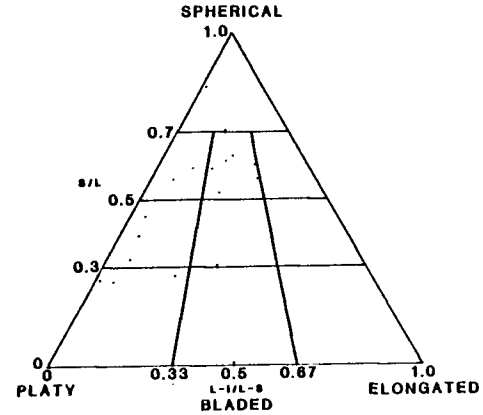

K-32(MUNCIE CREEK) - PB

Figure 26. Shape data for Stark and "Dawson" Shales.

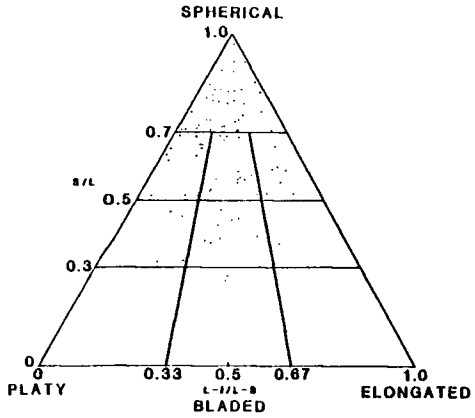

TOTAL STARK - S(B)

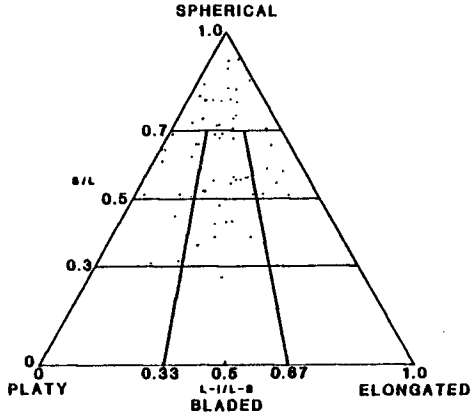

DSW(STARK) - SB

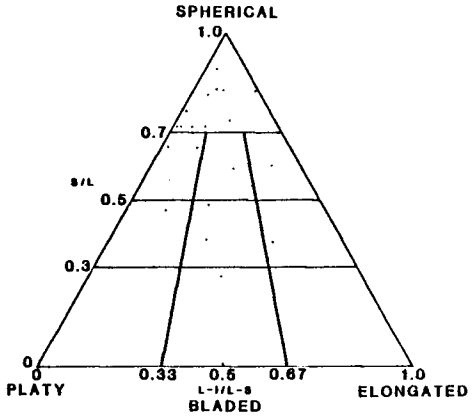

TSK(STARK) - S

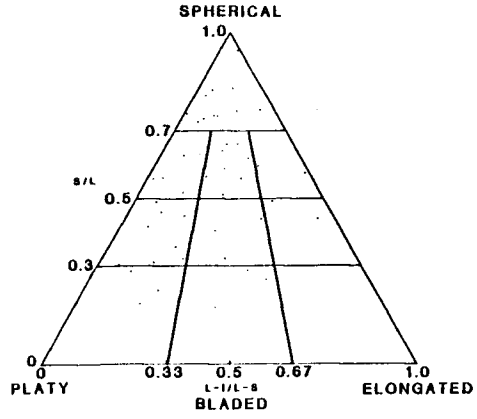

TOTAL "DAWSON" - SB

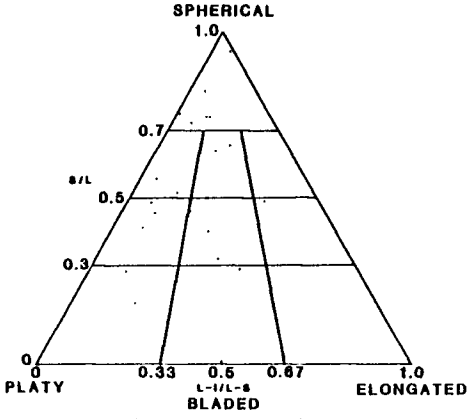

ODC("DAWSON") - SP

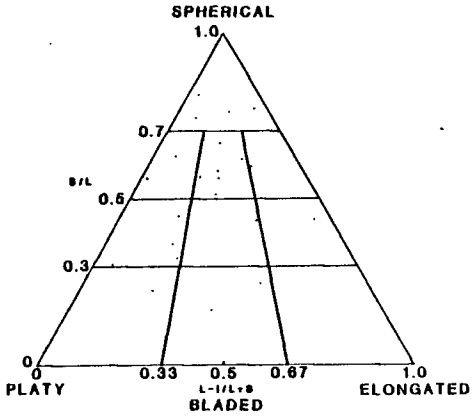

MVSW("DAWSON") - B(PS)

Figure 27. Shape data for Tacket Shale.

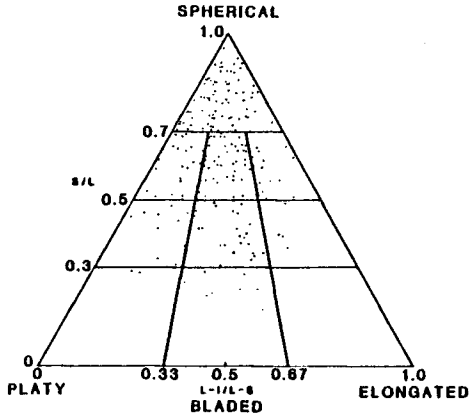

TOTAL TACKET - SB

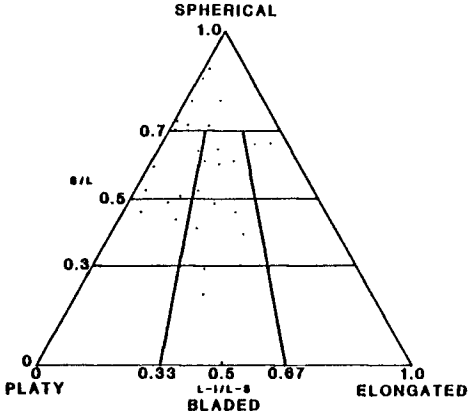

OHC(TACKET) - SB

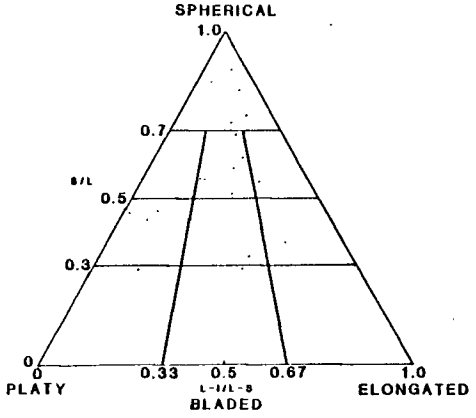

K-57(TACKET) - B(PS)

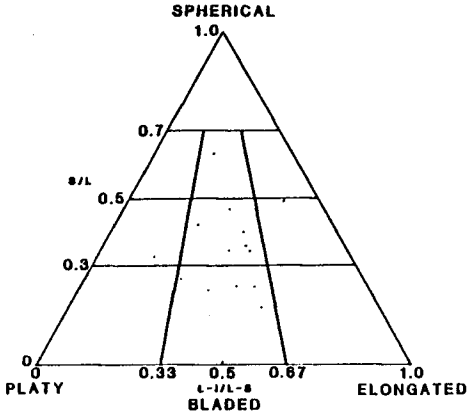

PCC(TACKET) - B

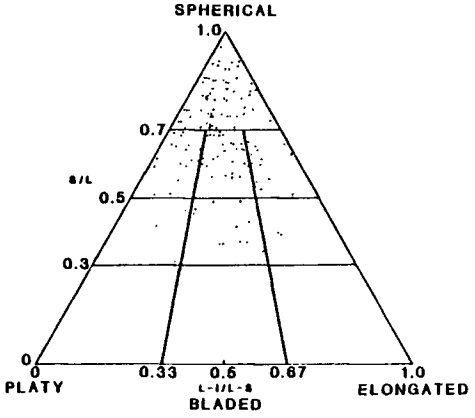

WLTN(TACKET) - SB

Figure 28. Shape data for Lake Neosho Shale.

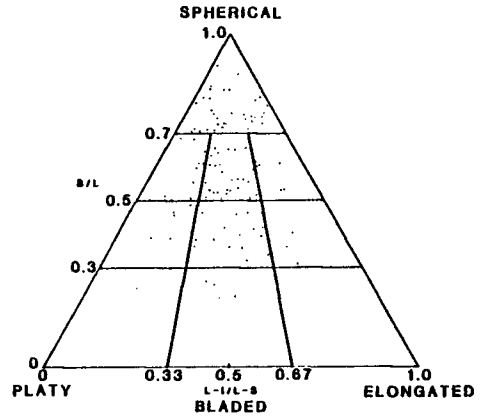

TOTAL LAKE NEOSHO - SB

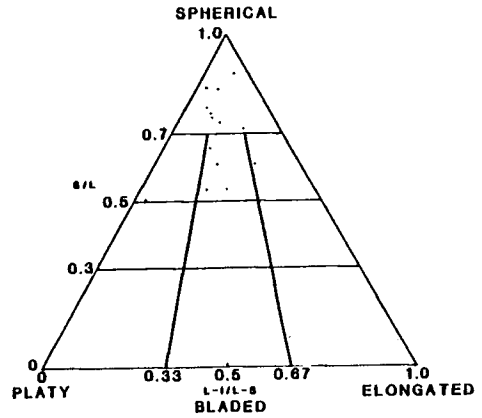

NCSL(LAKE NEOSHO) - S(B)

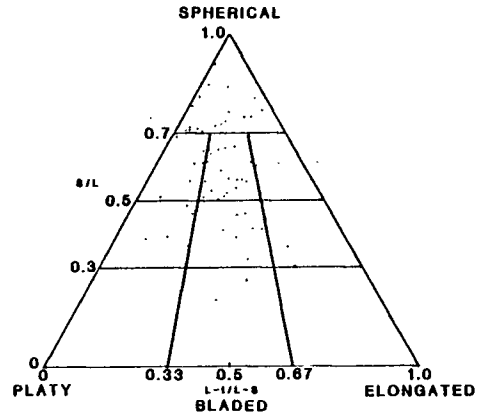

KBQ(LAKE NEOSHO) - SB

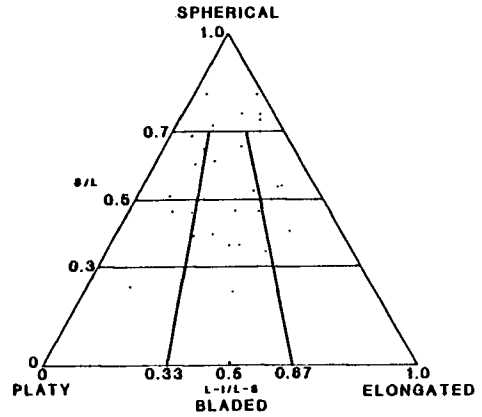

OWHB(LAKE NEOSHO) - BS

Figure 29. Shape data for Anna Shale.